WAVE PROPAGATION IN A SEMI-INFINITE, CYLINDRICAL, ORTHOTROPIC MEMBRANE

by

James J. Brickley, Jr.

Thesis submitted to the Graduate Faculty of the
Virginia Polytechnic Institute and State University
in partial fulfillment of the requirements for the degree of
MASTER OF SCIENCE
in
Engineering Mechanics

APPROVED:

J. Counts, Chairman

Carl T. Herakovich

F. J. Maher

April, 1972

Blacksburg, Virginia

ACKNOWLEDGMENTS

The author wishes to express his gratitude to his advisor, who suggested the topic and provided guidance in overcoming perplexing problems. The author also wishes to express his thanks to the other members of his committee for their constructive criticisms. To go thanks for the teaching assistantship which, besides giving invaluable experience, helped provide support during part of the author's program. Finally, the typist, is acknowledged for her efforts which resulted in ninety-nine percent accuracy on the first try!

TABLE OF CONTENTS

TABLE OF CONTENTS - continued

TABLE OF CONTENTS - continued

LIST OF FIGURES

LIST OF FIGURES - continued

NOMENCLATURE

$A_{ij}, B_{ij}, C_{ij} (i,j = 1,2,\ldots,n)$	Constants in second order operator, D_{ij}
c_0	A wave speed $\left\{ \equiv \sqrt{\frac{E_{LL}}{\rho(1-\nu_{LT}\nu_{TL})}} \right\}$
c_1, c_2	Wave speed of axial and torsional waves respectively
$C_i^s (i = 1,2;\ s = +,-)$	Characteristics
$D_{ij} (i,j = 1,2,\ldots,n)$	General second order operator
E_{LL}, E_{TT}	Young's modulus parallel and perpendicular to fibers respectively (orthotropic)
G_{LT}	Shear modulus (orthotropic)
h	Membrane thickness
p	General designation for roots of wave speed equation $\left(= \frac{dT}{dX}\right)$
$p_i^s (i = 1,2;\ s = +,-)$	The four roots of the wave speed equation
p.ℓ.c.	Primary leading characteristic
$Q^*_{ij} (i,j = 1,2,3)$	Stiffness elements relating stresses and strains parallel and perpendicular to fibers
$\bar{Q}_{ij} (i,j = 1,2,3)$	Stiffness elements relating stresses and strains parallel and perpendicular to cylinder axis
$Q_{ij} (i,j = 1,2,3)$	Non-dimensional form of $\bar{Q}_{ij} \left(= \bar{Q}_{ij}/\rho c_0^2\right)$
r	Radial coordinate
R	Cylinder radius measured to midsurface

R_i	Right hand term in difference equations (also, in wave equations written with second order operator)
S_{12}	Non-dimensional shear stress
s^+, s^-	Normalized coordinates for parabolic interpolation
s.ℓ.c.	Secondary leading characteristic
t	Time
T	Non-dimensional time (= tc_o/R)
T_{max}	Cut-off time for numerical solution
ΔT	Time interval for numerical solution
ΔT^*	A time interval (= $\Delta T[2-\zeta]$)
$u_i (i = 1,2,3)$	Displacements in x,ϕ, and r directions
$U_i (i = 1,2,3)$	Non-dimensional form of u_i (= u_1/R, u_2, u_3/R) (n.b. u_2 is already non-dimensional)
$\dot{u}_i (i = 1,2,3)$	Particle velocities in x, ϕ, and r directions
$\dot{U}_i (i = 1,2,3)$	Non-dimensional form of $\dot{u}_i$ (= $\dot{u}_1/c_o$, $\dot{u}_2 R/c_o$, $\dot{u}_3/c_o$)
$\ddot{u}_i (i = 1,2,3)$	Particle accelerations in x, ϕ, and r directions
$\ddot{U}_i (i = 1,2,3)$	Non-dimensional form of $\ddot{u}_i$ (= $\ddot{u}_1 R/c_o^2$, $\ddot{u}_2 R^2/c_o^2$, $\ddot{u}_3 R/c_o^2$)
$u_i' (i = 1,2,3)$	First partial spatial derivatives of displacements in x,ϕ, and r directions
$U_i' (i = 1,2,3)$	Non-dimensional form of u_i' (= u_1', $u_2' R$, u_3')
$u_i'' (i = 1,2)$	Second partial spatial derivatives of displacements in x and ϕ directions

$U_i''(i = 1,2)$	Non-dimensional form of $u_i''(= u_1''R, u_2''R^2)$
$[U_1']$, $[\dot{U}_1]$, $[U_2']$, $[\dot{U}_2]$	Jumps in first derivatives
V_0	Velocity of cylinder before impact
$W_i(i = 1,2,3,4,5)$	Coefficients involved in coordinate transformation of stiffness matrix
x	Axial coordinate
X	Non-dimensional form of $x(= x/R)$
ΔX	Spatial interval for numerical solution
α,β,γ	Angles characterizing grid
$\underset{\sim}{\gamma}$	Shear strain
$\varepsilon_x,\varepsilon_\phi$	Normal strains
ζ	Proportioning factor in grid
$\eta,\kappa,\lambda,\mu,\xi$	General form of coefficients in compatibility relations
$\eta_i^s,\kappa_i^s,\lambda_i^s,\mu_i^s(i = 1,2;\ s=+,-)$	Specific coefficients in compatibility relations, obtained upon substitution of p_i^s
θ	Helix angle for fibers
ν_{12},ν_{21}	Orthotropic Poisson's ratios
ρ	Mass density of membrane material
σ_x,σ_ϕ	Normal stresses
τ	Shear stress
Υ	$\equiv \frac{1}{2}\left(\frac{Q_{11} + Q_{33}}{Q_{11}Q_{33} - Q_{13}^2}\right)$

ϕ	Angular coordinate
χ	$\equiv \frac{1}{2}\left(Q_{11} + Q_{33}\right)$

I. INTRODUCTION AND LITERATURE REVIEW

Increased use of composite, anisotropic materials for structural elements has enhanced the importance of obtaining mathematical solutions for some of the boundary value problems which are encountered. An impact loading on the end of a circular, cylindrical shell is a dynamic problem encountered in many situations. If the cylinder is constructed from composite, anisotropic material, one straightforward arrangement is a series of helically wound fibers embedded in a matrix. Such a material will, in general, exhibit orthotropic behavior, which introduces an element of asymmetry to the problem, since neither of the principal directions is parallel to the shell axis.

The purpose of this effort is to develop and solve a set of equations for the impact response of a semi-infinite, cylindrical membrane shell of helically-oriented, linearly-elastic, orthotropic material. No closed-form solution has ever been obtained for the simpler problem of an isotropic, cylindrical membrane including radial inertia. Therefore, it is obvious that an approximate technique is required to obtain a solution for the orthotropic case. Of several available techniques, the method of characteristics stands out as best suited for this problem. Because the paths chosen in the time-space plane are lines of discontinuity in the first derivatives, the compatibility relations reduce to simpler form and the pertinent parameters, such as wavespeeds, become readily apparent.

With these considerations in mind, compatibility relations and wave speeds are developed from the equations of motion and constitutive relations, and the problem is solved numerically using the method of characteristics. Because of the asymmetry mentioned above, the mathematical formulation yields two sets of linear characteristics with different slopes. The second set is associated with a torsional disturbance which is absent in symmetrical configurations.

The method of characteristics was applied to the Timoshenko beam by Leonard and Budiansky[1] [11]. Other investigators [9,10] considered impact of semi-infinite, cylindrical, membrane shells of isotropic elastic or viscoelastic material, utilizing Laplace transforms to obtain solutions of the simplified equations. Spillers [1] extended the latter investigation to include bending, rotary inertia and transverse shear (Timoshenko shell), but turned to the method of characteristics for solutions, since the equations became too complex to be dealt with by transform methods. Subsequently, Chou and Mortimer [4] outlined a general procedure for the solution of elastic wave problems involving one space variable by the method of characteristics. Counts and Bennett [2], on the other hand, showed how a dynamic finite element technique could be used to obtain solutions for both semi-infinite and finite cylindrical and conical membrane shells.

---

[1]Numbers in brackets refer to the appended list of references.

Thus far, the work, whether assuming elastic or viscoelastic behavior, membrane or Timoshenko shell, finite or semi-infinite extent, was based upon isotropic material properties. Reuter [3] presented a solution for impact of a semi-infinite cylindrical membrane shell of helically-oriented orthotropic material, but neglected circumferential stress, in order to obtain a solution using transforms. The same author [8] subsequently analyzed the same shell including radial inertia, but for a harmonic disturbance for which he obtained stress and displacement ratios and dispersion curves.

Using the method of characteristics to analyze the impact of a cylindrical membrane shell of helically-oriented, orthotropic material, including radial inertia, is an important advance beyond the efforts outlined above. The aforementioned analysis, developed in ensuing chapters, introduces not just an additional method for obtaining a solution already available by other means, but results which are more comprehensive than those obtained previously. The method of characteristics is able to handle numerically the resulting set of three second order, partial differential equations with coupled terms, which defy solution in closed form.

II. FORMULATION OF THE PROBLEM

Equations of Motion

In Figure 1, the cylindrical coordinates indicated are x in the axial direction, ϕ in the circumferential direction, and r in the radial direction. The equation of motion will be written in each of these coordinate directions. For this purpose u_1, u_2, and u_3 are defined as the particle displacements in the x, ϕ, and r directions. σ_x, σ_ϕ, ε_x, and ε_ϕ represent the normal stresses and strains in the directions indicated by the subscripts. Finally, τ and γ represent the shear stress and strain.

Summing forces in the x direction for the differential shell segment in Figure 2 yields the following equation

$$\frac{\partial \sigma_x}{\partial x} dx(hRd\phi) = (hRd\phi dx)\ \rho\ddot{u}_1 \tag{2.1}$$

where ρ is the mass density of the shell material and $\ddot{u}_1$ is the second partial temporal derivative of the axial displacement (i.e., the axial particle acceleration). Simplification leads to

$$\sigma_x' = \rho\ddot{u}_1 \tag{2.2}$$

where the prime indicates differentiation with respect to x. Equation 2.2 is the equation of motion in the axial direction. Similar equations are obtained in the other two coordinate directions. They are

$$\tau' = R\rho\ddot{u}_2 \tag{2.3}$$

in the circumferential direction and

$$-\sigma_\phi = R\rho\ddot{u}_3 \tag{2.4}$$

in the radial direction. It should be noted here that u_2 is angular particle displacement, which is expressed in radians and is therefore dimensionless. In their present form, the equations of motion are valid for any material, but the assumption of orthotropic properties will be introduced below.

Strain-Displacement and Constitutive Equations

The following expressions relate the strains to the displacements in the cylinder:

$$\varepsilon_x = u_1' \tag{2.5}$$

$$\varepsilon_\phi = u_{3/R} \tag{2.6}$$

$$\text{and } \gamma = Ru_2' \tag{2.7}$$

where, again, primes indicate differentiation with respect to x. Furthermore, the equations listed below relate the stresses to the strains for an orthotropic material.

$$\sigma_x = \bar{Q}_{11}\,\varepsilon_x + \bar{Q}_{12}\,\varepsilon_\phi + \bar{Q}_{13}\,\gamma \tag{2.8}$$

$$\sigma_\phi = \bar{Q}_{21}\,\varepsilon_x + \bar{Q}_{22}\,\varepsilon_\phi + \bar{Q}_{23}\,\gamma \tag{2.9}$$

$$\text{and } \tau = \bar{Q}_{31}\,\varepsilon_x + \bar{Q}_{32}\,\varepsilon_\phi + \bar{Q}_{33}\,\gamma \tag{2.10}$$

where the $\bar{Q}_{ij}$'s represent stiffness coefficients, which will be explained in the section on stiffness coefficients in terms of material properties.

Substituting equations 2.5-7 into equations 2.8-10, the expressions relating stresses to displacements are

$$\sigma_x = \bar{Q}_{11}\,u_1' + \bar{Q}_{12}\,\frac{u_3}{R} + \bar{Q}_{13}\,Ru_2' \tag{2.11}$$

$$\sigma_\phi = \bar{Q}_{21}\, u_1' + \bar{Q}_{22}\, \frac{u_3}{R} + \bar{Q}_{23}\, Ru_2' \tag{2.12}$$

$$\text{and} \quad \tau = \bar{Q}_{31}\, u_1' + \bar{Q}_{32}\, \frac{u_3}{R} + \bar{Q}_{33}\, Ru_2' \tag{2.13}$$

Wave Equations

The following equations result from substitution of equations 2.11-13 into the equations of motion, 2.2-4, and rearrangement.

$$u_1'' - \frac{\rho}{\bar{Q}_{11}}\, \ddot{u}_1 = -\frac{1}{R}\frac{\bar{Q}_{12}}{\bar{Q}_{11}}\, u_3' - R\,\frac{\bar{Q}_{13}}{\bar{Q}_{11}}\, u_2'' \tag{2.14}$$

$$u_2'' - \frac{\rho}{\bar{Q}_{33}}\, \ddot{u}_2 = -\frac{1}{R}\frac{\bar{Q}_{31}}{\bar{Q}_{33}}\, u_1'' - \frac{1}{R^2}\frac{\bar{Q}_{32}}{\bar{Q}_{33}}\, u_3' \tag{2.15}$$

$$\ddot{u}_3 = -\frac{1}{R^2}\,\frac{\bar{Q}_{22}}{\rho}\, u_3 - \frac{1}{R}\frac{\bar{Q}_{21}}{\rho}\, u_1' - \frac{\bar{Q}_{23}}{\rho}\, u_2' \tag{2.16}$$

Non-Dimensionalization of the Wave Equations

The following definitions are made:

$$U_1 = \frac{u_1}{R} \tag{2.17}$$

$$U_2 = u_2 \tag{2.18}$$

$$U_3 = \frac{u_3}{R} \tag{2.19}$$

$$X = \frac{x}{R} \tag{2.20}$$

$$T = t\,\frac{c_o}{R} \tag{2.21}$$

$$c_o = \sqrt{\frac{E_{LL}}{\rho(1-\nu_{LT}\nu_{TL})}} \tag{2.22}$$

where [1]c_o is a wave speed, E_{LL} is the longitudinal Young's modulus (i.e., parallel to the fibers), and ν_{LT} and ν_{TL} are the orthotropic Poisson's ratios. Furthermore,

$$Q_{ij} = \frac{\bar{Q}_{ij}}{\rho c_o^2} \qquad \text{for } i=1,2,3 \text{ and } j=1,2,3 \tag{2.23}$$

Utilizing the above definitions, expressions can be derived for the derivatives in the wave equations in terms of the new non-dimensional variables. For example,

$$u_1' = \frac{\partial u_1}{\partial x} = \frac{\partial u_1}{\partial X} \cdot \frac{\partial X}{\partial x} = \frac{\partial U_1}{\partial X} \cdot \frac{\partial u_1}{\partial U_1} \cdot \frac{\partial X}{\partial x} = \frac{\partial U_1}{\partial X} \cdot R \cdot \frac{1}{R} = \frac{\partial U_1}{\partial X} = U_1'$$

$$u_1'' = \frac{\partial^2 u_1}{\partial x^2} = \frac{\partial}{\partial x}\left(\frac{\partial U_1}{\partial X}\right) = \frac{\partial}{\partial X}\left(\frac{\partial U_1}{\partial X}\right) \cdot \frac{\partial X}{\partial x} = \frac{\partial^2 U_1}{\partial X^2} \cdot \frac{1}{R} = \frac{1}{R} U_1''$$

Through a similar process, all the following expressions can be produced.

$$u_1'' = \frac{U_1''}{R} \tag{2.24}$$

$$\ddot{u}_1 = \frac{c_o^2}{R} \ddot{U}_1 \tag{2.25}$$

$$u_2'' = \frac{U_2''}{R^2} \tag{2.26}$$

---

[1] c_o is a constant, representing a wave speed, which is introduced for the purpose of non-dimensionalization. The value assigned, $\sqrt{\frac{E_{LL}}{\rho(1-\nu_{LT}\nu_{TL})}}$, has been chosen because it causes the greatest simplification.

$$\ddot{u}_2 = \frac{c_o^2}{R^2} \ddot{U}_2 \tag{2.27}$$

$$\ddot{u}_3 = \frac{c_o^2}{R} \ddot{U}_3 \tag{2.28}$$

$$u_1' = U_1' \tag{2.29}$$

$$u_2' = \frac{U_2'}{R} \tag{2.30}$$

$$u_3' = U_3' \tag{2.31}$$

Substituting equations 2.24-31 and equations 2.23 into equations 2.14-16, the wave equations are reduced to

$$U_1'' - \frac{1}{Q_{11}} \ddot{U}_1 + \frac{Q_{13}}{Q_{11}} U_2'' = - \frac{Q_{12}}{Q_{11}} U_3' \tag{2.32}$$

$$U_2'' - \frac{1}{Q_{33}} \ddot{U}_2 + \frac{Q_{13}}{Q_{33}} U_1'' = - \frac{Q_{32}}{Q_{33}} U_3' \tag{2.33}$$

$$\text{and } \ddot{U}_3 = - Q_{21} U_1' - Q_{23} U_2' - Q_{22} U_3 \tag{2.34}$$

Stiffness Coefficients in Terms of Material Properties

The macro-mechanics approach is assumed in developing expressions for the properties of the shell material. That is, the fiber-resin geometry is ignored and the lamina is assumed to be a homogeneous, orthotropic medium. The ensuing formulation parallels that of Ashton, Halpin, and Petit [5].

The constitutive relations can be written in matrix notation as

$$\begin{bmatrix} \sigma_L \\ \sigma_T \\ \tau_{LT} \end{bmatrix} = \begin{bmatrix} Q^*_{11} & Q^*_{12} & 0 \\ Q^*_{12} & Q^*_{22} & 0 \\ 0 & 0 & 2Q^*_{33} \end{bmatrix} \begin{bmatrix} \varepsilon_L \\ \varepsilon_T \\ \gamma_{LT}/2 \end{bmatrix} \tag{2.35}$$

where L and T represent respectively the directions parallel and perpendicular to the fibers in the surface of the membrane, and 3 represents the direction of the outward normal to the surface. In this reference system, the components of the Hooke's law or stiffness matrix are

$$\begin{aligned} Q^*_{11} &= E_{LL}/(1-\nu_{LT}\nu_{TL}) \\ Q^*_{22} &= E_{TT}/(1-\nu_{LT}\nu_{TL}) \\ Q^*_{12} &= \nu_{TL}\, E_{LL}/(1-\nu_{LT}\nu_{TL}) = \nu_{LT}\, E_{TT}/(1-\nu_{LT}\nu_{TL}) \\ Q^*_{33} &= G_{LT} \\ Q^*_{13} &= Q^*_{23} = 0 \end{aligned} \tag{2.36}$$

There are four independent elastic constants: the Young's moduli parallel and perpendicular to the fibers in the surface, E_{LL} and E_{TT}: the shear modulus, G_{LT}; the major Poisson's ratio, ν_{LT}. The fifth constant can be expressed as

$$\nu_{TL} = \nu_{LT} \frac{E_{TT}}{E_{LL}} \tag{2.37}$$

The constitutive relations can be transformed to the x, ϕ, r reference system shown in Figures 1 and 2. Equations 2.8-10 represent these transformed relations. Using the form given by Tsai and Pagano [7], the stiffness coefficients are written

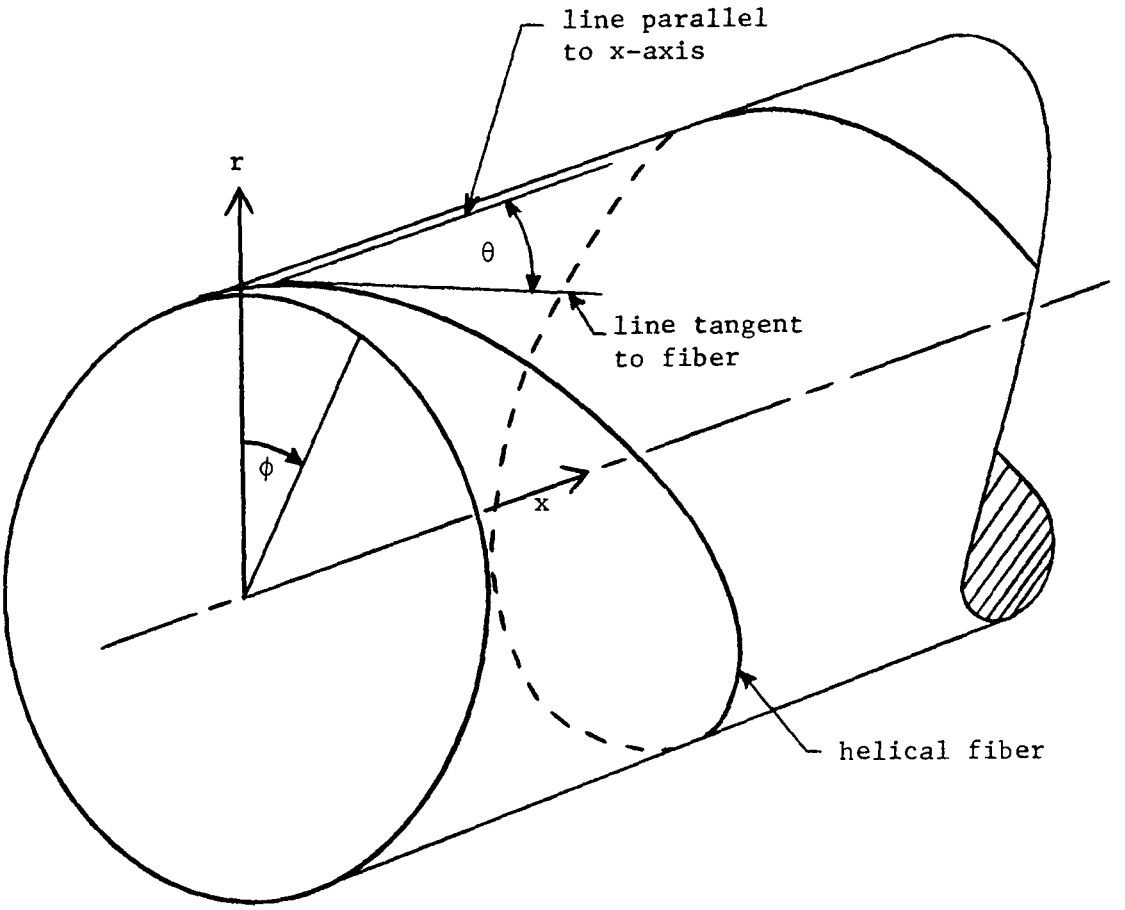

Figure 1. Section of a circular cylindrical membrane, indicating coordinate directions and orientation of a representative fiber with helix angle θ.

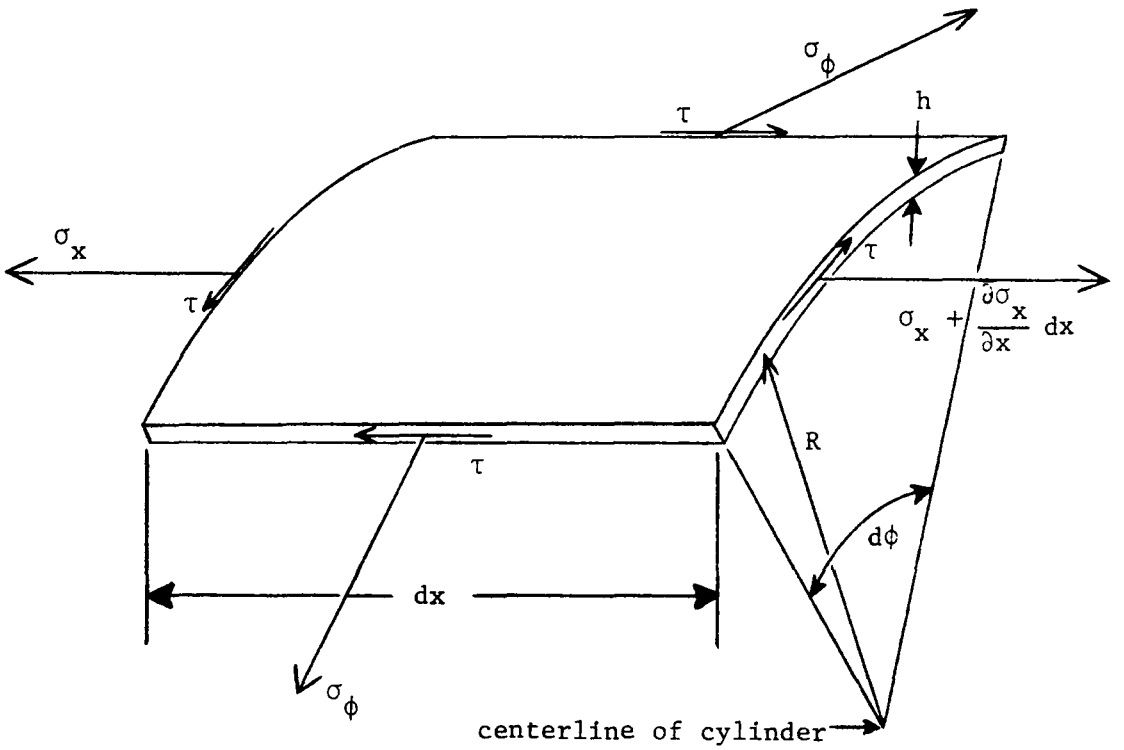

Figure 2. Free-body diagram of a differential segment of the membrane with a thickness, h, and a mid-surface radius of R.

$$\bar{Q}_{11} = W_1 + W_2 \cos(2\theta) + W_3 \cos(4\theta)$$

$$\bar{Q}_{22} = W_1 - W_2 \cos(2\theta) + W_3 \cos(4\theta)$$

$$\bar{Q}_{12} = W_4 - W_3 \cos(4\theta) \tag{2.38}$$

$$\bar{Q}_{33} = W_5 - W_3 \cos(4\theta)$$

$$\bar{Q}_{13} = -\frac{1}{2} W_2 \sin(2\theta) - W_3 \sin(4\theta)$$

$$\bar{Q}_{23} = -\frac{1}{2} W_2 \sin(2\theta) + W_3 \sin(4\theta)$$

where

$$W_1 = \frac{1}{8}(3Q^*_{11} + 3Q^*_{22} + 2Q^*_{12} + 4Q^*_{33})$$

$$W_2 = \frac{1}{2}(Q^*_{11} - Q^*_{22})$$

$$W_3 = \frac{1}{8}(Q^*_{11} + Q^*_{22} - 2Q^*_{12} - 4Q^*_{33}) \tag{2.39}$$

$$W_4 = \frac{1}{8}(Q^*_{11} + Q^*_{22} + 6Q^*_{12} - 4Q^*_{33})$$

$$W_5 = \frac{1}{8}(Q^*_{11} + Q^*_{22} - 2Q^*_{12} + 4Q^*_{33})$$

and W_1, W_4, and W_5 are invariant with respect to θ, the helix angle shown in Figure 1. Finally, the $\bar{Q}_{ij}$'s are non-dimensionalized via equations 2.23 to yield the Q_{ij}'s .

III. DEVELOPMENT OF WAVE-SPEED AND COMPATIBILITY RELATIONSHIPS

Expressions for the axial propagation speeds of the longitudinal and torsional waves, as well as compatibility relations valid in the characteristic directions must be developed before a numerical solution can be formulated. The requisite equations can be written as functions of the material properties and helix angle through consideration of the non-dimensional wave equations (2.32-34). The procedure followed here is that of Chou and Perry [6].

As a first step it is useful to introduce a general second order operator, D_{ij}, where

$$D_{ij} = A_{ij} \frac{\partial^2}{\partial x^2} + B_{ij} \frac{\partial^2}{\partial x \partial t} + C_{ij} \frac{\partial^2}{\partial t^2} \qquad (i,j = 1,2,\ldots,n) \qquad (3.1)$$

This is written in terms of two independent variables, x and t, which in this case represent axial position and time respectively. Utilizing this operator, a system of wave equations can be expressed as

$$\sum_{j=1}^{n} D_{ij} U_j = R_i \qquad (i = 1,2,\ldots,n) \qquad (3.2)$$

where the U_j's are displacements and the R_i's are functions of the displacements and their first derivatives. Equations 2.32-34, expressed in the foregoing notation, take the form

$$D_{11} U_1 + D_{12} U_2 = R_1 \qquad (3.3)$$

$$D_{21} U_1 + D_{22} U_2 = R_2 \qquad (3.4)$$

$$D_{33} U_3 = R_3 \qquad (3.5)$$

Now, according to Chou [6], equations 3.3 and 3.4 are hyperbolic and equation 3.5 is a parabolic equation, weakly coupled to the previous two. The term "weakly" indicates that no second derivatives are involved in the coupling. The weakly-coupled equation can be analyzed independently, and the two hyperbolic equations can be considered as a separate system for which characteristics can be found.

A system of two second order equations in two independent variables (e.g., position and time) can be written in general form as

$$A_1 U_1'' + B_1 U_2'' + C_1 \ddot{U}_1 + D_1 \ddot{U}_2 + E_1 \dot{U}_1' + F_1 \dot{U}_2' = R_1 \tag{3.6}$$

$$A_2 U_1'' + B_2 U_2'' + C_2 \ddot{U}_1 + D_2 \ddot{U}_2 + E_2 \dot{U}_1' + F_2 \dot{U}_2' = R_2 \tag{3.7}$$

where primes and dots indicate differentiation with respect to position and time respectively. In order to express equations 2.32 and 2.33 in this form, the following definitions must be made:

$$A_1 = 1;\ B_1 = \frac{Q_{13}}{Q_{11}};\ C_1 = -\frac{1}{Q_{11}};\ D_1 = E_1 = F_1 = 0;\ R_1 = -\frac{Q_{12}}{Q_{11}} U_3' \tag{3.8}$$

$$A_2 = \frac{Q_{13}}{Q_{33}};\ B_2 = 1;\ C_2 = 0;\ D_2 = -\frac{1}{Q_{33}};\ E_2 = F_2 = 0;\ R_2 = -\frac{Q_{32}}{Q_{33}} U_3'$$

Next, a series of differential relations, valid along any curve in the X - T plane can be written as follows:

$$dU_1' = U_1'' \, dX + \dot{U}_1' \, dT \tag{3.9}$$

$$d\dot{U}_1 = \dot{U}_1' \, dX + \ddot{U}_1 \, dT \tag{3.10}$$

$$dU_2' = U_2'' \, dX + \dot{U}_2' \, dT \tag{3.11}$$

$$d\dot{U}_2 = \dot{U}_2' \, dX + \ddot{U}_2 \, dT \tag{3.12}$$

Equations 3.6, 3.7, and 3.9-12 form a set of six equations in six unknowns, namely the six possible second derivatives. This set may be expressed in matrix notation as

$$\begin{bmatrix} A_1 & B_1 & C_1 & D_1 & E_1 & F_1 \\ A_2 & B_2 & C_2 & D_2 & E_2 & F_2 \\ 0 & 0 & dT & 0 & dX & 0 \\ 0 & 0 & 0 & dT & 0 & dX \\ dX & 0 & 0 & 0 & dT & 0 \\ 0 & dX & 0 & 0 & 0 & dT \end{bmatrix} \begin{bmatrix} U''_1 \\ U''_2 \\ \ddot{U}_1 \\ \ddot{U}_2 \\ \dot{U}'_1 \\ \dot{U}'_2 \end{bmatrix} = \begin{bmatrix} R_1 \\ R_2 \\ d\dot{U}_1 \\ d\dot{U}_2 \\ dU'_1 \\ dU'_2 \end{bmatrix} \tag{3.13}$$

The foregoing equations are all valid throughout the X - T plane. It is necessary, at this stage, to write expressions which are valid for points in the X - T plane at which there are jumps (i.e., discontinuities) in the <u>first</u> derivatives. The locus of all such points is the network of characteristics which describes the dynamic response of the membrane. Indeterminacy of the second derivatives at a given point is a necessary and sufficient condition for jumps in the first derivatives to occur at that point. The indeterminacy condition is satisfied in equations 3.13 if the determinant of the coefficient matrix and the determinants of the six possible matrices formed by replacing one column in the coefficient matrix with the right hand column vector are all simultaneously set equal to zero (in other words, if application of Kramer's Rule yields solutions of zero-over-zero for all the second derivatives).

Expressions for Wave Speeds

Setting the determinant of the coefficient matrix in equations 3.13 equal to zero after substitution of equations 3.8, the following is obtained:

$$(dT)^4 - \frac{1}{Q_{33}}(dX)^2(dT)^2 - \frac{Q_{13}^2}{Q_{11}Q_{33}}(dT)^4 - \frac{1}{Q_{11}}(dX)^2(dT)^2 + \frac{1}{Q_{11}Q_{33}}(dX)^4 = 0 \tag{3.14}$$

Dividing through by $(dX)^4$ and applying the quadratic rule yields

$$\left(\frac{dT}{dX}\right)^2 = \frac{1}{2}\left(\frac{Q_{11}+Q_{33}}{Q_{11}Q_{33}-Q_{13}^2}\right)\left[1 \pm \sqrt{1 - \frac{4(Q_{11}Q_{33}-Q_{13}^2)}{(Q_{11}+Q_{33})^2}}\right] \tag{3.15}$$

It can be shown, for the feasible range of material properties and for all helix angles, that

$$(Q_{11}Q_{33} - Q_{13}^2) > 0$$

$$(Q_{11} + Q_{33}) > 0 \tag{3.16}$$

$$\text{and } \frac{4(Q_{11}Q_{33} - Q_{13}^2)}{(Q_{11} + Q_{33})^2} < 1$$

Under these conditions, equation 3.15 yields four real, distinct roots, p(p = dT/dX). Let

$$T = \frac{1}{2}\,\frac{Q_{11} + Q_{33}}{Q_{11}Q_{33} - Q_{13}^2} \tag{3.17}$$

$$\text{and } \chi = \frac{1}{2}(Q_{11} + Q_{33}) \tag{3.18}$$

Then, the four roots can be written

$$
\begin{aligned}
p_1^+ &= + \left\{T\left[1 - (1 - 1/T\chi)^{1/2}\right]\right\}^{1/2} \\
p_1^- &= - \left\{T\left[1 - (1 - 1/T\chi)^{1/2}\right]\right\}^{1/2} \\
p_2^+ &= + \left\{T\left[1 + (1 - 1/T\chi)^{1/2}\right]\right\}^{1/2} \\
p_2^- &= - \left\{T\left[1 + (1 - 1/T\chi)^{1/2}\right]\right\}^{1/2}
\end{aligned}
\tag{3.19}
$$

These are the slopes of the four sets of characteristics in the X - T plane. The magnitude of the first two roots is smaller than that of the second two roots. Since these magnitudes represent the inverses of the wave speeds, the first two roots are indicative of the greater wave speed and are, consequently, associated with the longitudinal wave. Similarly, the last two roots, indicating the lesser wave speed, are associated with the torsional wave.

Compatibility Relations

Next, if the right hand vector is substituted for the first column of the coefficient matrix in equations 3.13 and the determinant of the resulting matrix is set equal to zero, the following is obtained:

$$
\begin{aligned}
&\left[-\frac{1}{Q_{11}Q_{33}} + p^2\frac{1}{Q_{11}}\right] dU_1' + \left[p\frac{1}{Q_{11}Q_{33}} - p^3\frac{1}{Q_{11}}\right] \dot{dU}_1 \\
&+ \left[-p^2\frac{Q_{13}}{Q_{11}Q_{33}}\right] dU_2' + \left[p^3\frac{Q_{13}}{Q_{11}Q_{33}}\right] \dot{dU}_2 \\
&= \left[p^2\frac{Q_{12}}{Q_{11}Q_{33}}\, dU_3' + p^4\left(-\frac{Q_{12}}{Q_{11}} + \frac{Q_{13}Q_{32}}{Q_{11}Q_{33}}\right) U_3'\right] dX
\end{aligned}
\tag{3.20}
$$

where $p = \frac{dT}{dX}$. Substitution of the roots, p_1^+, p_1^-, p_2^+, and p_2^-, into equation 3.20 yields four compatibility relationships valid along the four types of characteristics. Replacing each of the second through sixth columns of the coefficient matrix by the right hand vector in equation 3.13 yields five additional matrices. Setting the determinants of these matrices equal to zero produces five more equations of the form of equation 3.20 which, upon insertion of the four roots, generate additional compatibility relationships. However, as Chou asserts [6]: "It can be shown that after substitution of any root $\frac{dT}{dX}$ into any two of the six equations ... if the two equations contain the same differentials (any or all of $d\dot{U}_1$, dU_1', $d\dot{U}_2$, dU_2', or dX) then the two equations produce one identical compatibility relation." In the present case, it turns out that each of the six equations produces the same four compatibility relations. Thus, the four independent compatibility relations can be formulated by simply substituting each of equations 3.19 into equation 3.20.

If, in equation 3.20, the "dX term" is shifted to the left hand side and the equation is divided through by the coefficient of dU_1', the following can be written:

$$dU_1' + \eta d\dot{U}_1 + \kappa dU_2' + \lambda d\dot{U}_2 + \mu U_3' \, dX = 0 \tag{3.21}$$

where

$$\eta = \frac{p - p^3 Q_{33}}{p^2 Q_{33} - 1} \tag{3.22}$$

$$\kappa = \frac{-p^2 Q_{13}}{p^2 Q_{33} - 1} \tag{3.23}$$

$$\lambda = \frac{p^3 Q_{13}}{p^2 Q_{33} - 1} \tag{3.24}$$

$$\mu = \frac{-p^2 Q_{12} + p^4 (Q_{12}Q_{33} - Q_{13}Q_{32})}{p^2 Q_{33} - 1} \tag{3.25}$$

but $$U_3' = \frac{\partial U_3}{\partial X} = \frac{\partial U_3}{\partial T} \cdot \frac{dT}{dX} = \dot{U}_3 \frac{dT}{dX} \tag{3.26}$$

Substituting equation 3.26 into equation 3.21 yields

$$dU_1' + \eta d\dot{U}_1 + \kappa dU_2' + \lambda d\dot{U}_2 + \mu \dot{U}_3 \, dT = 0 \tag{3.27}$$

where it should be noted that the coefficients are simply functions of the material properties and the helix angle.

By substituting the roots, from equations 3.19, for p in equations 3.22-25, four sets of coefficients are obtained for use in equation 3.27. The four equations produced can be expressed in matrix notation as

$$\begin{bmatrix} 1 & \eta_1^+ & \kappa_1^+ & \lambda_1^+ & \mu_1^+ dT \\ 1 & \eta_1^- & \kappa_1^- & \lambda_1^- & \mu_1^- dT \\ 1 & \eta_2^+ & \kappa_2^+ & \lambda_2^+ & \mu_2^+ dT \\ 1 & \eta_2^- & \kappa_2^- & \lambda_2^- & \mu_2^- dT \end{bmatrix} \begin{bmatrix} dU_1' \\ d\dot{U}_1 \\ dU_2' \\ d\dot{U}_2 \\ \dot{U}_3 \end{bmatrix} = \begin{bmatrix} 0 \\ 0 \\ 0 \\ 0 \end{bmatrix} \tag{3.28}$$

where $\eta_1^+ = \eta(p)\Big|_{p = p_1^+}$, etc.

---

[1]To solve these equations uniquely, a fifth equation is required. This is obtained from the radial motion equation as developed in Chapter V beginning with equation 5.17.

Cases of Degeneracy

0° and 90° Helix Angles. Substituting $\theta = 0°$ or 90° into the expression for $\bar{Q}_{13}$ (equations 2.38) gives

$$\bar{Q}_{13} = 0 \quad (\theta = 0°, 90°)$$

Then, from equations 2.23

$$Q_{13} = 0 \quad (\theta = 0°, 90°)$$

Substituting this into equations 3.23-24 yields

$$\kappa = \lambda = 0 \quad (\theta = 0°, 90°)$$

Thus, no matter what value of p is used, the third and fourth columns of the coefficient matrix in equations 3.28 are all zeros. The solutions for the four differentials and radial velocity ($\dot{U}_3$) are, therefore, indeterminate.

Isotropy. If the shell material is assumed to be isotropic,

$$E_{LL} = E_{TT} = E$$

$$\nu_{LT} = \nu_{TL} = \nu$$

$$G_{LT} = G = \frac{E}{2(1+\nu)}$$

Using these relations in equations 2.36, and solving for W_2 and W_3 in equations 2.39 results in

$$W_2 = W_3 = 0 \quad \text{(isotropic)}$$

From equations 2.38 and equations 2.23, this condition produces

$$Q_{13} = 0$$

As in the case of 0° and 90° helix angles, the foregoing indicates indeterminate solutions for equations 3.28.

All of these degenerate cases are ones in which the solution is uncoupled. That is, a normal stress input at the end of the cylinder generates a longitudinal wave, but no coupled torsional wave. Although the general formulation, as it stands, will not yield solutions for these special cases, equations which produce solutions for them can be developed using the same procedure presented here.

For the cases of 0° and 90° helix angles, if the definition is made that

$$\xi = \frac{p^3 Q_{11} - p}{1 - p^2 Q_{11}} \quad , \tag{3.29}$$

two compatibility relations can be written as follows:

$$dU_1' + \eta d\dot{U}_1 + \mu \dot{U}_3 dT = 0 \quad (\theta = 0°, 90°) \tag{3.30}$$

$$dU_2' + \xi d\dot{U}_2 = 0 \quad (\theta = 0°, 90°) \tag{3.31}$$

For the 0° and 90° cases, these replace equation 3.27. Notice that there is no coupling of terms between equations 3.30 and 3.31. Furthermore, the wave speed equation is

$$p^4 - \frac{Q_{11} + Q_{33}}{Q_{11}Q_{33}} p^2 + \frac{1}{Q_{11}Q_{33}} = 0 \quad (\theta = 0°, 90°) \tag{3.32}$$

which has roots

$$
\begin{aligned}
p_1^+ &= (Q_{11})^{-1/2} \\
p_1^- &= -(Q_{11})^{-1/2} \\
p_2^+ &= (Q_{33})^{-1/2} \\
p_2^- &= -(Q_{33})^{-1/2}
\end{aligned}
\tag{3.33}
$$

Substitution of p_1^+ and p_1^- into equation 3.30 yields two equations valid along the characteristics governing the longitudinal wave. Similarly, substitution of p_2^+ and p_2^- into equation 3.31 produces a pair of equations valid along torsional wave characteristics.

A parallel formulation can be done for the isotropic case, which has been solved several times in the literature. Further comment on these degenerate cases will be made in the presentation of results.

IV. FORMULATION OF JUMP RELATIONS AND BOUNDARY CONDITIONS

The X-T Plane

The four roots of equation 3.14, given in equations 3.19, are the values of $\frac{dT}{dX}$ which designate the characteristic directions in the X-T plane. They are, therefore, the inverses of the non-dimensionalized wave speeds.

$$c_1 = (p_1^+)^{-1} \tag{4.1}$$

$$c_2 = (p_2^+)^{-1} \tag{4.2}$$

where c_1 and c_2 are non-dimensionalized wave speeds. Henceforth in the development, the subscript "1" is used to designate entities related to the longitudinal compression wave, and the associated characteristics are referred to as primary. The subscript "2" pertains to the torsional wave, and the associated characteristics are called secondary characteristics.

An overall view of the grid formed by a set of equally spaced primary characteristics is shown in Figure 3. The primary leading characteristic shows the rate of advance of the longitudinal wave front. The secondary leading characteristic shows the progress of the lagging torsional disturbance. Within the grid, there are three groups of geometric figures which the characteristics and boundary delimit. Difference equations, necessary for the numerical solution, will be developed for interior quadrangles (e.g., (A)) and quadrangles lying

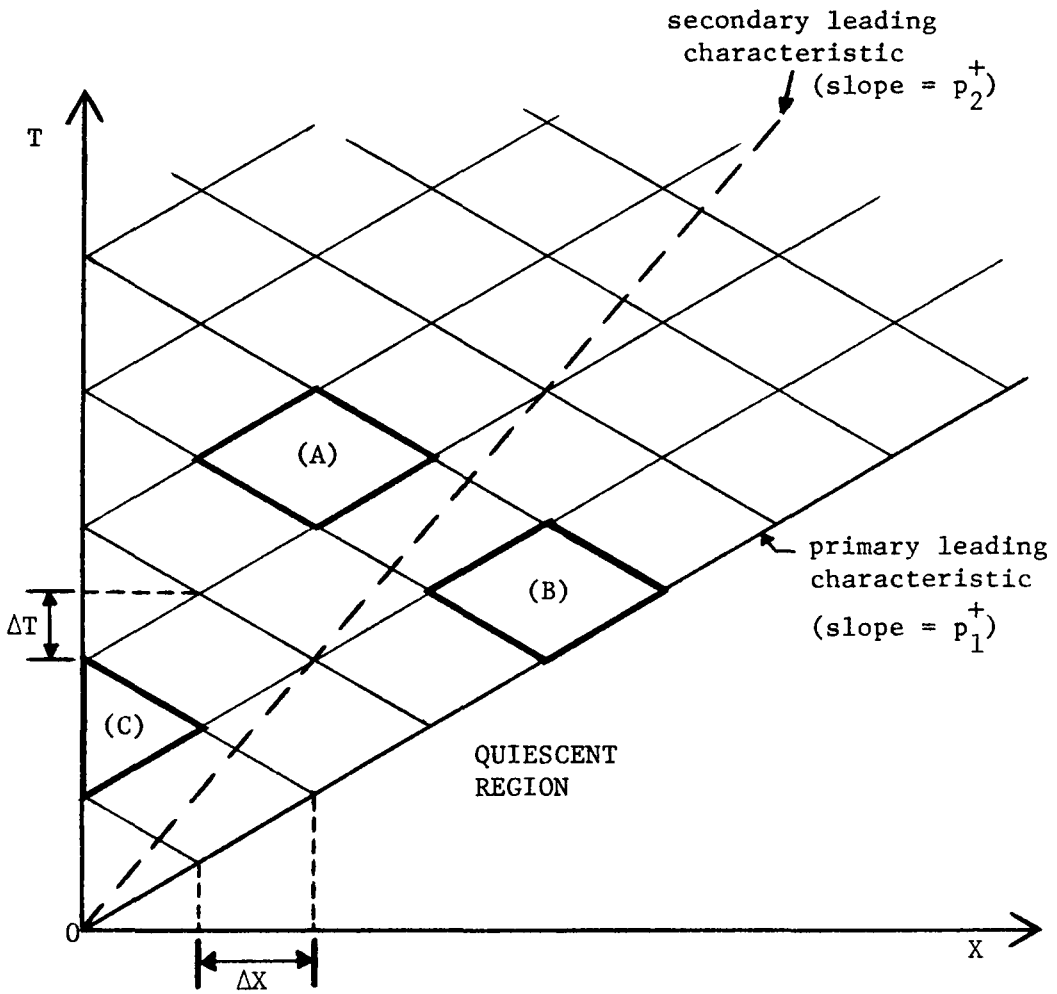

Figure 3. Portion of X-T plane showing primary and secondary leading characteristics and representative elements delimited by the characteristics.

along the primary leading characteristic (e.g., (B)), and then for triangles on the boundary (e.g., (C)). First, however, jump relations and boundary conditions must be formulated.

Jumps Across a Positive Primary Characteristic

As proven by Chou [4], there can be no jumps (discontinuities) in the first derivatives across lines in the X-T plane which are not characteristics. Relations, valid for jumps across a positive primary characteristic, are developed here using Chou's method. In Figure 4 are shown two positive primary characteristics (C_1^+) with a negative primary (C_1^-), negative secondary (C_2^-), and a positive secondary characteristic (C_2^+) which pass through a common point (A) on one of the C_1^+ characteristics.

The second of equations 3.28 can be integrated along C_1^- from A to B. The third and fourth of equations 3.28 can be integrated along C_2^+ from A to D and along C_2^- from A to C respectively. If $C_1^+(2)$ is then allowed to approach $C_1^+(1)$, in the limit as the distance between them goes to zero the aforementioned integrated expressions become

$$\begin{aligned}
&[U_1'] + \eta_1^- [\dot{U}_1] + \kappa_1^- [U_2'] + \lambda_1^- [\dot{U}_2] = 0 \quad \text{(across } C_1^+\text{)} \\
&[U_1'] + \eta_2^- [\dot{U}_1] + \kappa_2^- [U_2'] + \lambda_2^- [\dot{U}_2] = 0 \quad \text{(across } C_1^+\text{)} \qquad (4.3) \\
&[U_1'] + \eta_2^+ [\dot{U}_1] + \kappa_2^+ [U_2'] + \lambda_2^+ [\dot{U}_2] = 0 \quad \text{(across } C_1^+\text{)}
\end{aligned}$$

where [ ] means "the jump in." The validity of this operation depends, of course, on the fact that the coefficients of dT are finite.

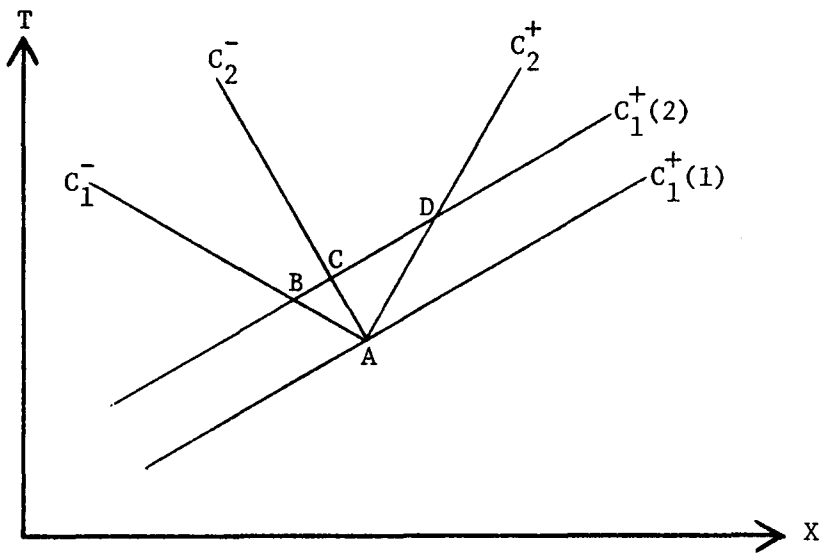

Figure 4. Two adjacent C_1^+ characteristics, showing a C_1^-, a C_2^-, and a C_2^+ characteristic which intersect one of the C_1^+ characteristics at a common point.

Jumps Across a Positive Secondary Characteristic

Through a process parallel to that used to develop equations 4.3, a set of equations for jumps across a positive secondary characteristic are obtained. They are

$$\begin{aligned}
&[U_1'] + \eta_1^- [\dot{U}_1] + \kappa_1^- [U_2'] + \lambda_1^- [\dot{U}_2] = 0 \quad (\text{across } C_2^+) \\
&[U_1'] + \eta_1^+ [\dot{U}_1] + \kappa_1^+ [U_2'] + \lambda_1^+ [\dot{U}_2] = 0 \quad (\text{across } C_2^+) \qquad (4.4) \\
&[U_1'] + \eta_2^- [\dot{U}_1] + \kappa_2^- [U_2'] + \lambda_2^- [\dot{U}_2] = 0 \quad (\text{across } C_2^+)
\end{aligned}$$

Propagation of Jumps Along Characteristics

The first of equations 3.28 is valid along all positive primary characteristics. If one C_1^+ characteristic approaches another C_1^+ characteristic, in the limit as the distance between them goes to zero the following is obtained:

$$d[U_1'] + \eta_1^+ d[\dot{U}_1] + \kappa_1^+ d[U_2'] + \lambda_1^+ d[\dot{U}_2] = 0 \quad (\text{along } C_1^+) \qquad (4.5)$$

Since equations 4.4 comprise three equations in four unknowns, any three of the jumps can be expressed in terms of a constant times the remaining jump. Such expressions can then be substituted into equation 4.5. Since the differential of a constant-times-a-jump is equal to the constant times the differential of the jump, the fact that equation 4.5 can be written entirely in terms of one jump variable indicates that the differential of that jump variable must be equal to zero. The same thing, of course, is true for the other three jump variables. Consequently, jumps propagate along C_1^+ characteristics

with constant magnitudes. A similar conclusion can be drawn for C_2^+ characteristics.

Boundary Conditions at the Wall

It will be seen, in the development of the difference equations in the next chapter, that two equations beyond the compatibility relations (equations 3.28) are required to obtain a solution at the wall. The first condition is self-evident. Once the semi-infinite cylinder has impacted the wall, the axial velocity of its end must be zero. Therefore,

$$\dot{U}_1\Big|_{X = 0} = 0 \quad (T \geq 0) \tag{4.6}$$

To provide a second condition, the shear stress is assumed to be zero at the wall. Non-dimensionalizing equation 2.13 by using equations 2.17-19, the following is obtained:

$$S_{12} = Q_{31}U_1' + Q_{33}U_2' + Q_{32}U_3$$

where S_{12} represents the non-dimensional shear stress. Thus, at the wall,

$$Q_{31}U_1' + Q_{33}U_2' + Q_{32}U_3 = 0 \quad (X = 0) \tag{4.7}$$

"Initial" Conditions

It is possible to begin the numerical solution along the X-axis (i.e., $T = 0$, $X > 0$) where all displacements and derivatives, except

the axial velocity, are zero. However, none of the aforementioned variables change value anywhere below the primary leading characteristic. Integration over this quiescent region (shown in Figure 3) would use computer time and increase numerical inaccuracy. Therefore, it is desirable to specify "initial" conditions along the primary leading characteristic, not the X-axis.

The velocity of the cylinder, just before impacting the wall, is defined as $-V_0$. It is designated a negative because the direction of wave propagation has been defined as positive (i.e., increasing X). Time zero is defined as immediately after impact. Thus, at the origin (X = 0, T = 0), a jump in axial velocity has just occurred and can be represented

$$[\dot{U}_1]_{\text{origin}} = 0 - (-V_0) = + V_0 \tag{4.8}$$

It has been shown that jumps propagate along C_1^+ and C_2^+ characteristics with constant magnitudes. Thus, jumps across the p.ℓ.c. at any point along its length are identical to the jumps across the p.ℓ.c. at the origin, and equations 4.3 are applicable in all such cases. In addition, equations 4.4 are valid for jumps across the secondary leading characteristic (s.ℓ.c.) at all points along its length, including the origin, and the jumps have identical values everywhere along the characteristic.

At this stage, it is useful to examine the situation at the origin more closely. The latter point is the only one in the X-T plane which lies on both the p.ℓ.c. and the s.ℓ.c. Therefore, the jump in any

variable at the origin must be the sum of its jumps across the p.ℓ.c. and the s.ℓ.c. Considering that U_1', U_2', and U_3 are all zero just <u>before</u> impact and that these three variables must satisfy equation 4.7 at the wall (and, therefore, at the origin) just <u>after</u> impact, the following obtains:

$$Q_{31}[U_1']_{\text{origin}} + Q_{33}[U_2']_{\text{origin}} + Q_{32}[U_3]_{\text{origin}} = 0 \qquad (4.9)$$

Jumps in the radial displacement, U_3, are not admissible, if continuity of the membrane surface is to be preserved. Therefore, setting the third term in equation 4.9 equal to zero and writing the remaining jumps in terms of their components across the p.ℓ.c. and the s.ℓ.c., yields

$$Q_{31}\left\{[U_1']_{\text{p.}\ell\text{.c.}} + [U_1']_{\text{s.}\ell\text{.c.}}\right\} + Q_{33}\left\{[U_2']_{\text{p.}\ell\text{.c.}} + [U_2']_{\text{s.}\ell\text{.c.}}\right\} = 0 \qquad (4.10)$$

The jump in equation 4.8 can also be split into two parts, as follows:

$$[\dot{U}_1]_{\text{p.}\ell\text{.c.}} + [\dot{U}_1]_{\text{s.}\ell\text{.c.}} = +V_0 \qquad (4.11)$$

There are, now, eight jump relations written in terms of eight variables. These include equations 4.3, 4.4, 4.10, and 4.11. If the velocity of the cylinder before impact, V_0, is set equal to unity to normalize the solution, the foregoing set of equations can be written in matrix notation as:

$$\begin{bmatrix} 1 & \eta_1^- & \kappa_1^- & \lambda_1^- & 0 & 0 & 0 & 0 \\ 1 & \eta_2^- & \kappa_2^- & \lambda_2^- & 0 & 0 & 0 & 0 \\ 1 & \eta_2^+ & \kappa_2^+ & \lambda_2^+ & 0 & 0 & 0 & 0 \\ 0 & 0 & 0 & 0 & 1 & \eta_1^- & \kappa_1^- & \lambda_1^- \\ 0 & 0 & 0 & 0 & 1 & \eta_1^+ & \kappa_1^+ & \lambda_1^+ \\ 0 & 0 & 0 & 0 & 1 & \eta_2^- & \kappa_2^- & \lambda_2^- \\ Q_{31} & 0 & Q_{33} & 0 & Q_{31} & 0 & Q_{33} & 0 \\ 0 & 1 & 0 & 0 & 0 & 1 & 0 & 0 \end{bmatrix} \begin{bmatrix} [U_1']_{p.\ell.c.} \\ [\dot{U}_1]_{p.\ell.c.} \\ [U_2']_{p.\ell.c.} \\ [\dot{U}_2]_{p.\ell.c.} \\ [U_1']_{s.\ell.c.} \\ [\dot{U}_1]_{s.\ell.c.} \\ [U_2']_{s.\ell.c.} \\ [\dot{U}_2]_{s.\ell.c.} \end{bmatrix} = \begin{bmatrix} 0 \\ 0 \\ 0 \\ 0 \\ 0 \\ 0 \\ 0 \\ 1 \end{bmatrix} \tag{4.12}$$

Since the radial wave equation, 2.34, is parabolic, the radial velocity experiences no jumps. Thus,

$$[\dot{U}_3]_{p.\ell.c.} = [\dot{U}_3]_{s.\ell.c.} = 0 \tag{4.13}$$

The values of the first derivatives assigned as "initial" conditions along the p.ℓ.c. are those which exist immediately after the jumps have occurred. Therefore,

$$(\dot{U}_1)_{p.\ell.c.} = -V_0 + [\dot{U}_1]_{p.\ell.c.} \tag{4.14}$$

Since the remaining first derivatives have zero values in the quiescent region, the values assigned to them along the p.ℓ.c. are identical to the values of their jumps across the p.ℓ.c.

The magnitudes of the jumps across the s.ℓ.c., as obtained from equations 4.12, are not needed as input in order to produce solutions. The jumps across the s.ℓ.c. are generated by the numerical integration and the values from equations 4.12 can be used to check the results of the integration.

V. DEVELOPMENT OF THE DIFFERENCE EQUATIONS

As indicated in the last chapter, difference equations are to be developed for each of the categories of geometrical figures (A, B, and C) delimited by the finite difference grid shown in Figure 3. These equations will, subsequently, provide the means to integrate numerically throughout the X-T plane and calculate the values of displacements, velocities, stresses, etc.

Quadrangles

Shown in Figure 5 is an interior quadrangle bounded by segments of four primary characteristics, designated C_1^+ and C_1^-. Since a set of characteristics can be drawn through any point in the X-T plane, secondary characteristics (C_2^+ and C_2^-) are drawn through point P and intersect the lower pair of primary characteristics at points M* and O*. From Figure 5, the following relations can be written:

(using equation 4.1) $$\beta = \arctan c_1 \tag{5.1}$$

(using equation 4.2) $$\alpha = \arctan c_2 \tag{5.2}$$

$$\gamma = \pi - \alpha - \beta \tag{5.3}$$

$$\overline{PN}^{1} = 2\Delta T \tag{5.4}$$

---

[1] $\overline{PN}$ represents the length of the line connecting points P and N. All such designations represent line lengths between two points.

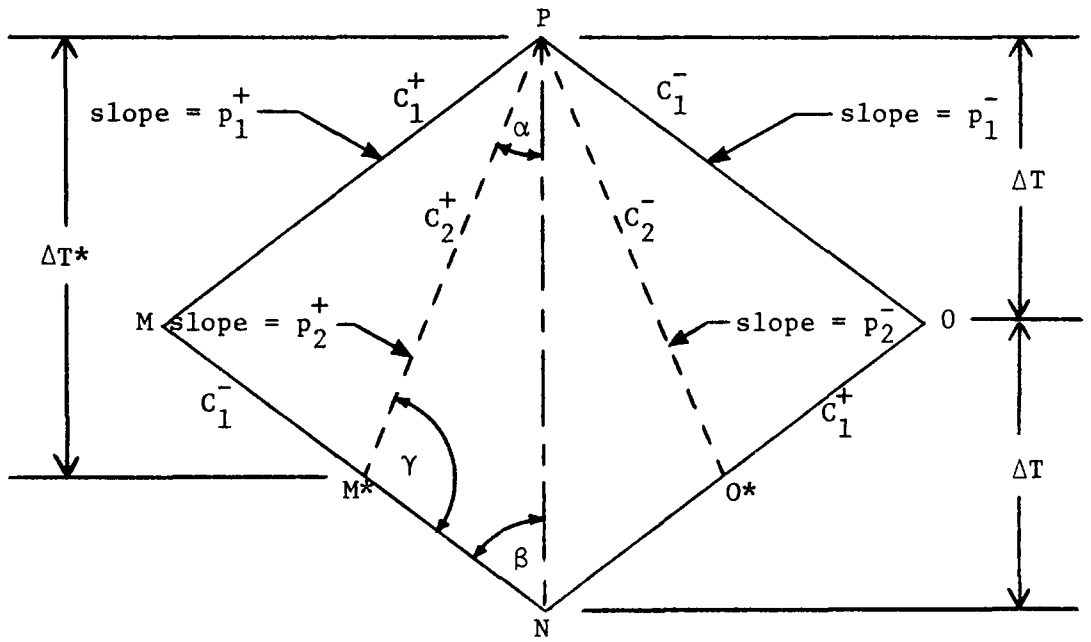

Figure 5. An interior quadrangle bounded by segments of four primary characteristics.

$$\overline{NM^*} = \overline{PN}\ \sin\alpha/\sin\gamma \tag{5.5}$$

$$\overline{NM} = \Delta T\ \sec\beta \tag{5.6}$$

$$\frac{\overline{NO^*}}{\overline{NO}} = \frac{\overline{NM^*}}{\overline{NM}}\ (= \zeta \text{ by definition}) \tag{5.7}$$

$$\zeta = \frac{2\ \sin\alpha\ \cos\beta}{\sin\gamma} \tag{5.8}$$

(using equations 5.4,5,8) $\Delta T^* = 2\Delta T - \overline{NM^*}\ \cos\beta = \Delta T(2-\zeta)$ (5.9)

Now, if the values of a function of X and T are known at points M, N, and O, the values at M* and O* can be found by linear interpolation using ζ.

$$(\ )_{M^*} = (\ )_N + \zeta[(\ )_M - (\ )_N] \tag{5.10}$$

$$(\ )_{O^*} = (\ )_N + \zeta[(\ )_O - (\ )_N] \tag{5.11}$$

where ( ) represents any one of the variables defined in the X-T plane (e.g., U_1', $\dot{U}_1$, etc). This is, of course, based upon the assumption that functions of X and T vary approximately linearly from N to M and N to O for ΔT sufficiently small. A further assumption is

$$\int_1^2 \dot{U}_3 dT \simeq \frac{(\dot{U}_3)_1 + (\dot{U}_3)_2}{2}\ \Delta T \tag{5.12}$$

for ΔT sufficiently small. Using these approximating assumptions, each of equation 3.28 can be integrated along the appropriate characteristic.

$$[(U_1')_P - (U_1')_M] + \eta_1^+ [(\dot{U}_1)_P - (\dot{U}_1)_M] + \kappa_1^+ [(U_2')_P - (U_2')_M]$$
$$+ \lambda_1^+ [(\dot{U}_2)_P - (\dot{U}_2)_M] + \frac{\mu_1^+}{2} [(\dot{U}_3)_M + (\dot{U}_3)_P]\ \Delta T = 0 \tag{5.13}$$

From O to P (along C_1^-),

$$[(U_1')_P - (U_1')_0] + \eta_1^- [(\dot{U}_1)_P - (\dot{U}_1)_0] + \kappa_1^- [(U_2')_P - (U_2')_0]$$

$$+ \lambda_1^- [(\dot{U}_2)_P - (\dot{U}_2)_0] + \frac{\mu_1^-}{2} [(\dot{U}_3)_0 + (\dot{U}_3)_P] \Delta T = 0 \tag{5.14}$$

From M* to P (along C_2^+),

$$[(U_1')_P - (U_1')_{M*}] + \eta_2^+ [(\dot{U}_1)_P - (\dot{U}_1)_{M*}] + \kappa_2^+ [(U_2')_P - (U_2')_{M*}]$$

$$+ \lambda_2^+ [(\dot{U}_2)_P - (\dot{U}_2)_{M*}] + \frac{\mu_2^+}{2} [(\dot{U}_3)_{M*} + (\dot{U}_3)_P] \Delta T* = 0 \tag{5.15}$$

From O* to P (along C_2^-),

$$[(U_1')_P - (U_1')_{O*}] + \eta_2^- [(\dot{U}_1)_P - (\dot{U}_1)_{O*}] + \kappa_2^- [(U_2')_P - (U_2')_{O*}]$$

$$+ \lambda_2^- [(\dot{U}_2)_P - (\dot{U}_2)_{O*}] + \frac{\mu_2^-}{2} [(\dot{U}_3)_{O*} + (\dot{U}_3)_P] \Delta T* = 0 \tag{5.16}$$

where equations 5.10-11 are used to calculate $(\ )_{M*}$ and $(\ )_{O*}$.

If the values of all the first derivatives are known at points M, N, and O and their values at M* and O* are calculated using equations 5.10-11, the only unknowns in equations 5.13-16 are the values of the derivatives at point P. However, since five such unknowns appear in the latter four equations, another equation is required. Equations 5.13-16 were derived from the two hyperbolic wave equations, equations 2.32-33. The additional equation is supplied by the radial wave equation, equation 2.34, which is parabolic. Thus, from equation 2.34

$$\frac{\partial}{\partial T}\dot{U}_3 = - Q_{21}U_1' - Q_{23}U_2' - Q_{22}U_3 \tag{5.17}$$

Remembering that

$$d\dot{U}_3 = \frac{\partial \dot{U}_3}{\partial T}\,dT + \frac{\partial \dot{U}_3}{\partial X}\,dX, \tag{5.18}$$

if a path is chosen along which X is a constant

$$d\dot{U}_3 = \frac{\partial \dot{U}_3}{\partial T}\,dT \quad (X = \text{constant}) \tag{5.19}$$

Using equation 5.19, equation 5.17 can be written

$$d\dot{U}_3 = (- Q_{21}U_1' - Q_{23}U_2' - Q_{22}U_3)\,dT \quad (X = \text{constant}) \tag{5.20}$$

ΔT is assumed sufficiently small to allow the approximation

$$\int_N^P (\,)dt \cong \frac{(\,)_N + (\,)_P}{2}\,(2\Delta T) \tag{5.21}$$

where ( ) represents U_1', U_2', U_3 or $\dot{U}_3$. Using equation 5.21, equation 5.20 can be written in finite difference form between points N and P as follows:

$$(\dot{U}_3)_P - (\dot{U}_3)_N = \left\{ - \frac{Q_{21}}{2}\left[(U_1')_N + (U_1')_P\right] - \frac{Q_{23}}{2}\left[(U_2')_N + (U_2')_P\right] - \frac{Q_{22}}{2}\left[(U_3)_N + (U_3)_P\right] \right\} 2\Delta T \tag{5.22}$$

Furthermore,

$$(U_3)_P = (U_3)_N + \int_N^P \dot{U}_3 dT \tag{5.23}$$

Using equation 5.21, this becomes

$$(U_3)_P = (U_3)_N + \left[\frac{(\dot{U}_3)_N + (\dot{U}_3)_P}{2}\right] 2\Delta T \tag{5.24}$$

Substituting equation 5.24 into equation 5.22 and rearranging terms leads to

$$^{2}[Q_{22}(\Delta T)^2 + 1]\ (\dot{U}_3)_P + [Q_{22}(\Delta T)^2 - 1]\ (\dot{U}_3)_N = \{ - Q_{21}[(U_1')_N + (U_1')_P] - Q_{23}\ [(U_2')_N + (U_2')_P] - 2Q_{22}(U_3)_N\}\ \Delta T \qquad (5.25)$$

Upon rearrangement, equations 5.13-16 and equation 5.25 yield, in matrix notation,

$$\begin{bmatrix} 1 & \eta_1^+ & \kappa_1^+ & \lambda_1^+ & \frac{\mu_1^+}{2}\Delta T \\ 1 & \eta_1^- & \kappa_1^- & \lambda_1^- & \frac{\mu_1^-}{2}\Delta T \\ 1 & \eta_2^+ & \kappa_2^+ & \lambda_2^+ & \frac{\mu_2^+}{2}\Delta T^* \\ 1 & \eta_2^- & \kappa_2^- & \lambda_2^- & \frac{\mu_2^-}{2}\Delta T^* \\ \Delta T & 0 & \frac{Q_{23}}{Q_{21}}\Delta T & 0 & \frac{Q_{22}}{Q_{21}}\Delta T^2 + \frac{1}{Q_{21}} \end{bmatrix} \begin{bmatrix} (U_1')_P \\ (\dot{U}_1)_P \\ (U_2')_P \\ (\dot{U}_2)_P \\ (\dot{U}_3)_P \end{bmatrix} = \begin{bmatrix} R_1 \\ R_2 \\ R_3 \\ R_4 \\ R_5 \end{bmatrix} \qquad (5.26)$$

---

[2]This equation could be divided through by ΔT. However, the $(\Delta T)^{-1}$ terms produced thereby cause problems in the computer solution. The equation, is therefore, left in its present form which is the one used in the computer program.

where

$$R_1 = (U_1')_M + \eta_1^+(\dot{U}_1)_M + \kappa_1^+(U_2')_M + \lambda_1^+(\dot{U}_2)_M - \frac{\mu_1^+}{2}\Delta T\ (\dot{U}_3)_M \tag{5.27}$$

$$R_2 = (U_1')_O + \eta_1^-(\dot{U}_1)_O + \kappa_1^-(U_2')_O + \lambda_1^-(\dot{U}_2)_O - \frac{\mu_1^-}{2}\Delta T\ (\dot{U}_3)_O \tag{5.28}$$

$$R_3 = (U_1')_{M*} + \eta_2^+(\dot{U}_1)_{M*} + \kappa_2^+(U_2')_{M*} + \lambda_2^+(\dot{U}_2)_{M*} - \frac{\mu_2^+}{2}\Delta T^*\ (\dot{U}_3)_{M*} \tag{5.29}$$

$$R_4 = (U_1')_{O*} + \eta_2^-(\dot{U}_1)_{O*} + \kappa_2^-(U_2')_{O*} + \lambda_2^-(\dot{U}_2)_{O*} - \frac{\mu_2^-}{2}\Delta T^*\ (\dot{U}_3)_{O*} \tag{5.30}$$

$$R_5 = -\Delta T(U_1')_N - \frac{Q_{23}}{Q_{21}}\Delta T(U_2')_N + \left(\frac{1}{Q_{21}} - \frac{Q_{22}}{Q_{21}}\Delta T^2\right)(\dot{U}_3)_N - \frac{2Q_{22}}{Q_{21}}(U_3)_N\,\Delta T \tag{5.31}$$

For any quadrangular element within the grid, if the values of all the first derivatives and the radial displacement (U_3) are known at the three lower vertices, equations 5.26 can be used to calculate the values of the first derivatives at the uppermost vertex. For quadrangles which lie along the primary leading characteristic, equations 5.26 are valid, but certain additional information is available. In such quadrangles, points N, O*, and O all lie on the p.ℓ.c. Therefore, the values of the first derivatives at these three points are immediately known from the "initial" conditions formulated in the last chapter. As indicated there, the values are identical for all points lying on the p.ℓ.c.

Triangles on the Boundary

Figure 6 represents a boundary triangle, an example of which has been designated C in Figure 3. One secondary characteristic can be drawn through point P as shown. Again, as in the case of quadrangles, compatibility equations can be integrated along appropriate characteristics and expressed in finite difference form. Between O and P, equation 5.14 is again valid, as is equation 5.16 between O* and P. However, imposing the boundary condition expressed in equation 4.6, $(\dot{U}_1)_P$ is set equal to zero in these two equations, yielding

$$[(U_1')_P - (U_1')_O] - \eta_1^-(\dot{U}_1)_O + \kappa_1^- [(U_2')_P - (U_2')_O] + \lambda_1^- [(\dot{U}_2)_P - (\dot{U}_2)_O] + \frac{\mu_1^-}{2} [(\dot{U}_3)_O + (\dot{U}_3)_P] \Delta T = 0 \quad (5.32)$$

and

$$[(U_1')_P - (U_1')_{O*}] - \eta_2^-(\dot{U}_1)_{O*} + \kappa_2^- [(U_2')_P - (U_2')_{O*}] + \lambda_2^- [(\dot{U}_2)_P - (\dot{U}_2)_{O*}] + \frac{\mu_2^-}{2} [(\dot{U}_3)_{O*} + (\dot{U}_3)_P] \Delta T^* = 0 \quad (5.33)$$

where equations 5.9 and 5.11 are used to calculate ΔT^* and $(\ )_{O*}$. The radial wave equation, expressed in finite difference form between points N and P (equation 5.25), provides a third relation. To obtain a fourth relation, the shear boundary condition at the wall (equation 4.07) is written for point P as follows:

$$Q_{31}(U_1')_P + Q_{33}(U_2')_P + Q_{32}(U_3)_P = 0 \quad (5.34)$$

Substituting for $(U_3)_P$ from equation 5.24,

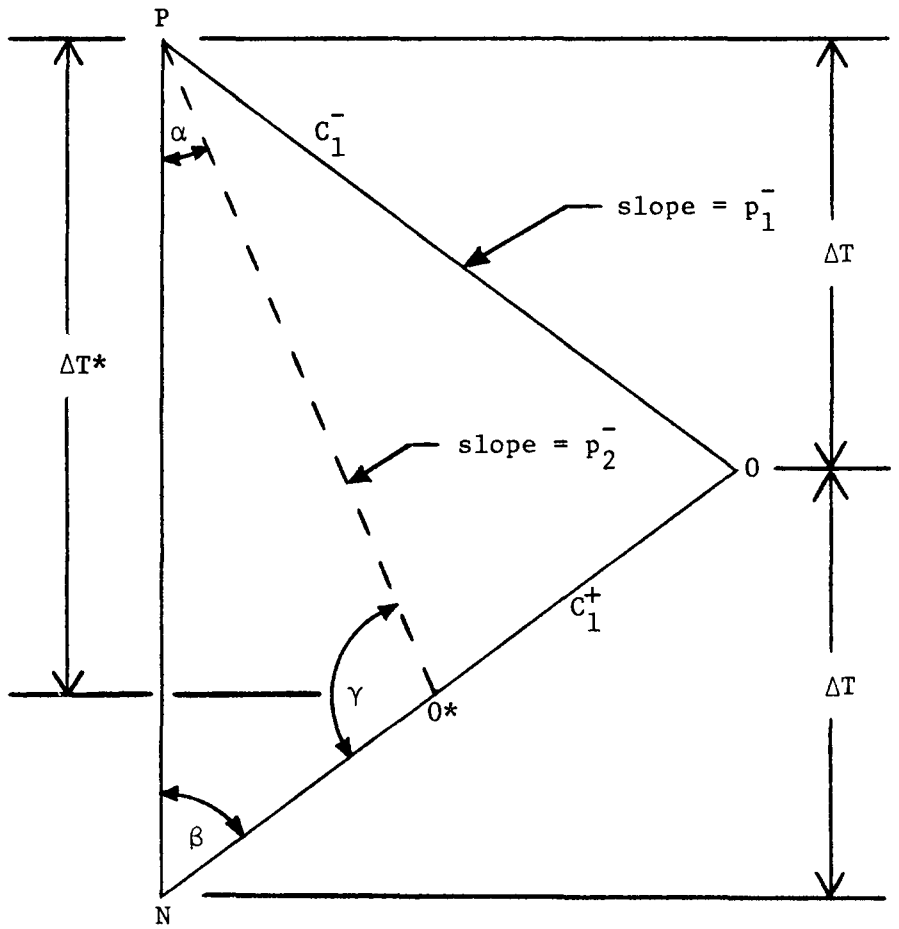

Figure 6. A triangle on the boundary delimited by segments of two primary characteristics and the time axis.

$$Q_{31}(U_1')_P + Q_{33}(U_2')_P + Q_{32}\,[(U_3)_N + (\dot{U}_3)_N\,\Delta T + (\dot{U}_3)_P\,\Delta T] = 0 \tag{5.35}$$

Rearranging equations 5.32, 33, 25, and 35, and writing them in matrix notation, yields

$$\begin{bmatrix} 1 & \kappa_1^- & \lambda_1^- & \frac{\mu_1^-}{2}\Delta T \\ 1 & \kappa_2^- & \lambda_2^- & \frac{\mu_2^-}{2}\Delta T^* \\ \Delta T & \frac{Q_{23}}{Q_{21}}\Delta T & 0 & \frac{Q_{22}}{Q_{21}}\Delta T^2 + \frac{1}{Q_{21}} \\ 1 & \frac{Q_{33}}{Q_{31}} & 0 & \frac{Q_{32}}{Q_{31}}\Delta T \end{bmatrix} \begin{bmatrix} (U_1')_P \\ (U_2')_P \\ (\dot{U}_2)_P \\ (\dot{U}_3)_P \end{bmatrix} = \begin{bmatrix} R_2 \\ R_4 \\ R_5 \\ R_6 \end{bmatrix} \tag{5.36}$$

where R_2, R_4, and R_5 are defined by equations 5.28, 30, and 31 respectively and

$$R_6 = -\frac{Q_{32}}{Q_{31}}\,[(U_3)_N + (\dot{U}_3)_N\,\Delta T] \tag{5.37}$$

For any triangular element at the wall boundary, if the values of all the first derivatives and the radial displacement (U_3) are known at the two lower vertices, equations 5.36 can be used to calculate the values of the first derivatives at the uppermost vertex.

VI. NUMERICAL INTEGRATION PROCEDURE

The order in which the integration is carried out is indicated by the numbering of the grid points in Figure 7. First, values are assigned at points 1 and 2 by using the "initial" conditions formulated in Chapter IV. Equations 5.36 then yield values for point 3. Axial velocity, $\dot{U}_1$, is zero at the latter point, as it is at all points for which X equals zero. Since point 4 is on the p.ℓ.c., the "initial" conditions again supply values there. With the values at 2, 3, and 4 known, equations 5.26 yield values for point 5. Knowing the values at 3 and 5, equations 5.36 are used to generate the values at point 6. Continuing this procedure, values are generated for all grid points. A cut-off time, T_{max}, indicated by the dashed line in Figure 7, is specified.

Convergence

The spacing of the grid is changed by specifying a different time interval, ΔT. As the grid is made finer, numerical convergence of the solution is assumed to have been achieved when plots of the output variables show no noticeable change for successive halvings of the time interval.

Secondary Jumps

Jumps in the first derivatives must occur across the secondary leading characteristic. These jumps are generated in the numerical soltions. Their relative magnitudes and locations (i.e., X and T coordi-

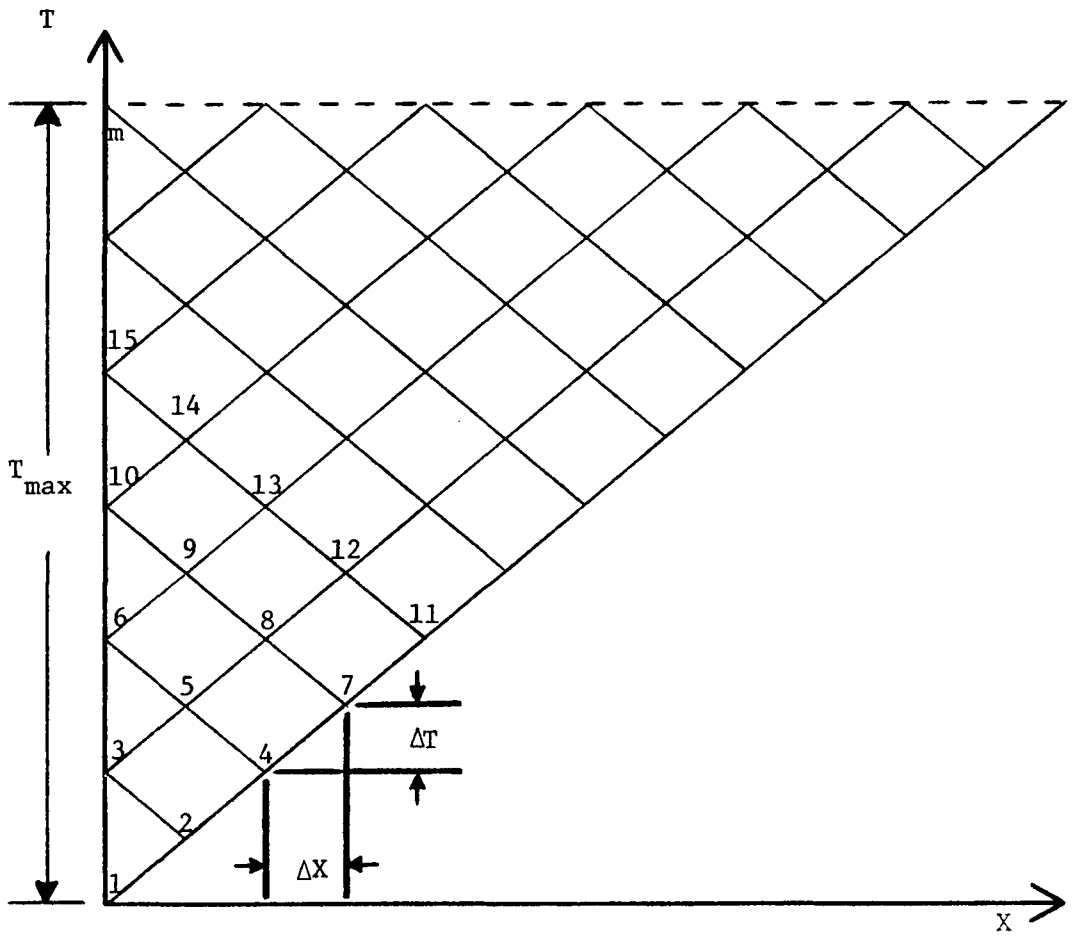

Figure 7. Portion of X-T plane indicating order of numerical integration. T_{max} is cut-off time for the solution.

nates) can be checked by utilizing the secondary jump relations and torsional wave speed.

Parabolic Interpolation

Values of the variables at points designated M* and O* in Figure 5 are calculated in the program using parabolic interpolation, not the linear interpolation specified in equations 5.10-11. The expressions used in this non-linear interpolation procedure, which refines the numerical integration somewhat, are developed below.

In Figure 8, a quadrangle from the grid is shown with part of two adjacent quadrangles. Two scales, defined so that the horizontal distance between adjacent grid points is unity, are indicated. S^+ is used for interpolating between N and O, and S^- for interpolating between N and M. Using these scales, ζ, as defined in equation 5.7, is the horizontal distance between N and O* or between N and M*. This sort of normalized system of measurement can be used, because the function values are being proportioned according to the relative spacing between the points. Thus,

$$S^+(M^-) = 0;\ S^+(N) = 1.0;\ S^+(O^*) = 1.0 + \zeta;\ S^+(O) = 2.0 \qquad (6.1)$$

If a function, f, is assumed to have a second degree variation between points M^- and O, it can be written

$$f = a^+(S^+)^2 + b^+(S^+) + C^+ \qquad (6.2)$$

where a^+, b^+, and c^+ are constants. Using equations 6.1 in equation 6.2 yields

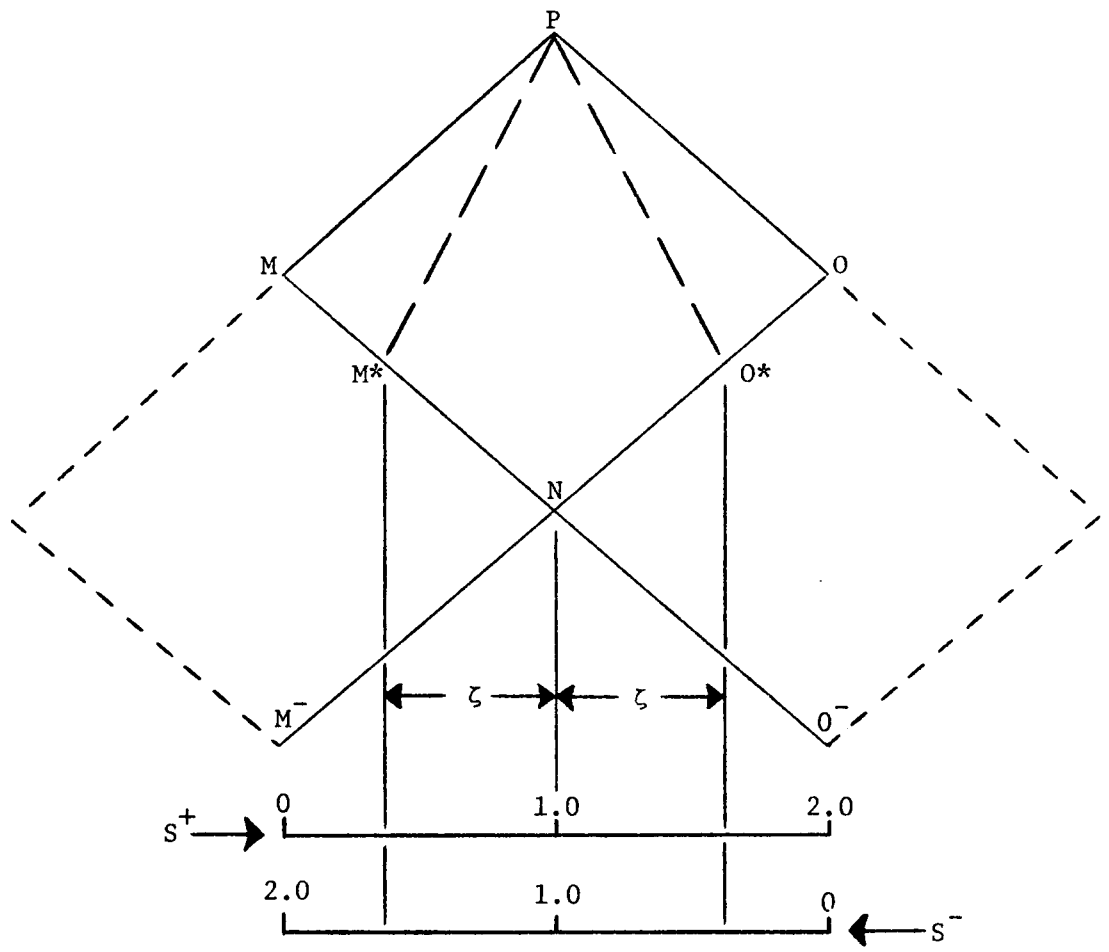

Figure 8. Normalized scales used in parabolic interpolation.

$$f_{M^-} = c^+$$
$$f_N = a^+ + b^+ + c^+ \tag{6.3}$$

and

$$f_O = 4a^+ + 2b^+ + c^+$$

where f_{M^-} represents the function evaluated at M^-, etc. Solving equation 6.3 for the coefficients gives

$$a^+ = \frac{f_{M^-} - 2f_N + f_O}{2}$$

$$b^+ = \frac{-3f_{M^-} + 4f_N - f_O}{2} \tag{6.4}$$

and

$$c^+ = f_{M^-}$$

Likewise, for interpolating between N and M, a function, f, can be defined by

$$f = a^-(S^-)^2 + b^-(S^-) + c^- \tag{6.5}$$

where

$$a^- = \frac{f_{O^-} - 2f_N + f_M}{2}$$

$$b^- = \frac{-3f_{O^-} + 4f_N - f_M}{2} \tag{6.6}$$

and

$$c^- = f_{O^-}$$

VII. DISCUSSION OF RESULTS AND CONCLUSIONS

Discussion of Results

With the exception of isotropic results, which will be discussed subsequently, no theoretical or experimental data are available to determine, by comparison, the validity of the numerical solutions. Therefore, beyond careful rechecking of the steps involved in producing the program, acceptability of the results must be based upon internal consistency. Since "initial" conditions along the p.ℓ.c. are imposed, they are of no use in checking results. Although two conditions are imposed at the wall (i.e. zero axial velocity and zero shear stress), the values of some of the variables are generated numerically and may be useful in comparisons.

The most convincing piece of evidence is contributed by the jumps in the first derivatives generated at the s.ℓ.c. by the numerical procedure. Equations 4.12 represent conditions that must be satisfied at the origin, which is, as stated previously, located on both the p.ℓ.c. and the s.ℓ.c. Since jumps propagate along the characteristics with constant magnitudes, the jump values resulting from simultaneous solution of equations 4.12 are valid everywhere along the leading characteristics. Although the jumps across the p.ℓ.c. are imposed in the boundary conditions, if any jumps appear at the s.ℓ.c., they are generated by numerical integration of the compatibility relations. Thus, if jumps occur in the output variables at the position of the s.ℓ.c. and they are of the magnitude and sign predicted by equations 4.12, there is ample reason to be confident of the procedure.

Oscillatory Behavior. There is one apparent problem encountered in the output. Oscillations are observed just behind the s.ℓ.c., an example of which is shown in Figure 9. The location of this oscillatory behavior is no surprise. It occurs immediately beyond the point at which the numerical procedure has generated a "nearly-infinite" gradient to model the jump in velocity at the secondary wavefront. Oscillations of this sort are found in all the output only for the variables which exhibit jumps at the s.ℓ.c. Radial velocity, for example, does not have jumps and exhibits no oscillations. Likewise, when negligibly small jumps occur, as in the "near-isotropic" case shown in Figure 10, no perceptible oscillations occur.

It would appear that use of a larger time interval for the numerical integration could eliminate the oscillations. This should certainly be true for some larger interval. However, solutions resulting from use of intervals two and four times greater than the one used in Figure 9 still contain oscillations, although they generate essentially identical values for all points outside of the oscillatory regions. Further enlargement of the interval does not seem to be a profitable route. The increased crudeness of the approximations would just make the overall results inaccurate. Likewise, decreasing the time interval does not result in a narrowed oscillatory region, although a smaller interval does cause an oscillation of higher frequency and greater amplitude. Thus, contraction of the interval is not promising.

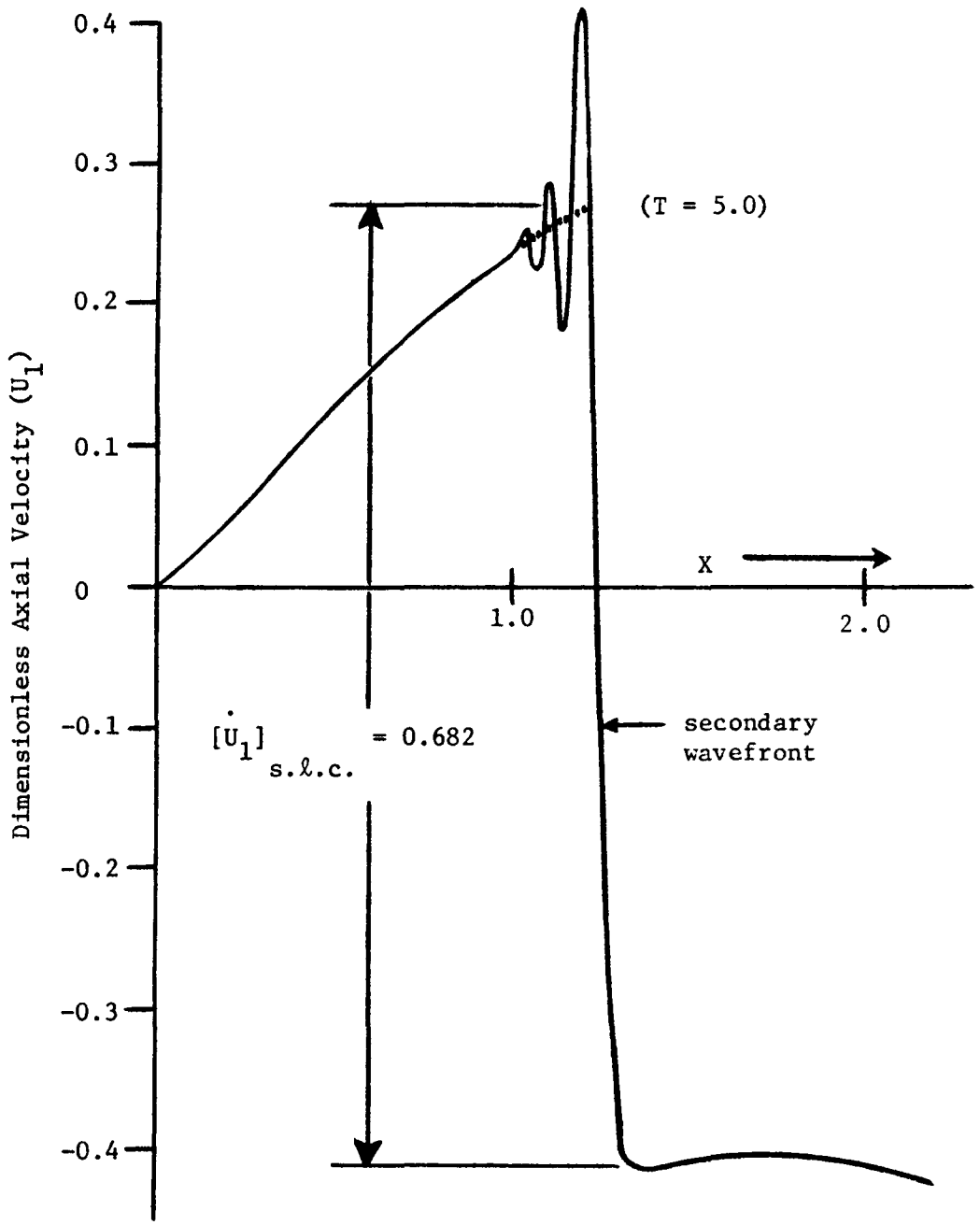

Figure 9. Spatial variation of non-dimensionalized axial velocity, showing oscillations behind the secondary wavefront ($\theta = 45°$; $E_{TT}/E_{LL} = 0.1$; $G_{LT}/E_{LL} = 0.0333...$; $\nu_{LT} = 0.3$; $T = 5.0$; $\Delta T = 0.00625$).

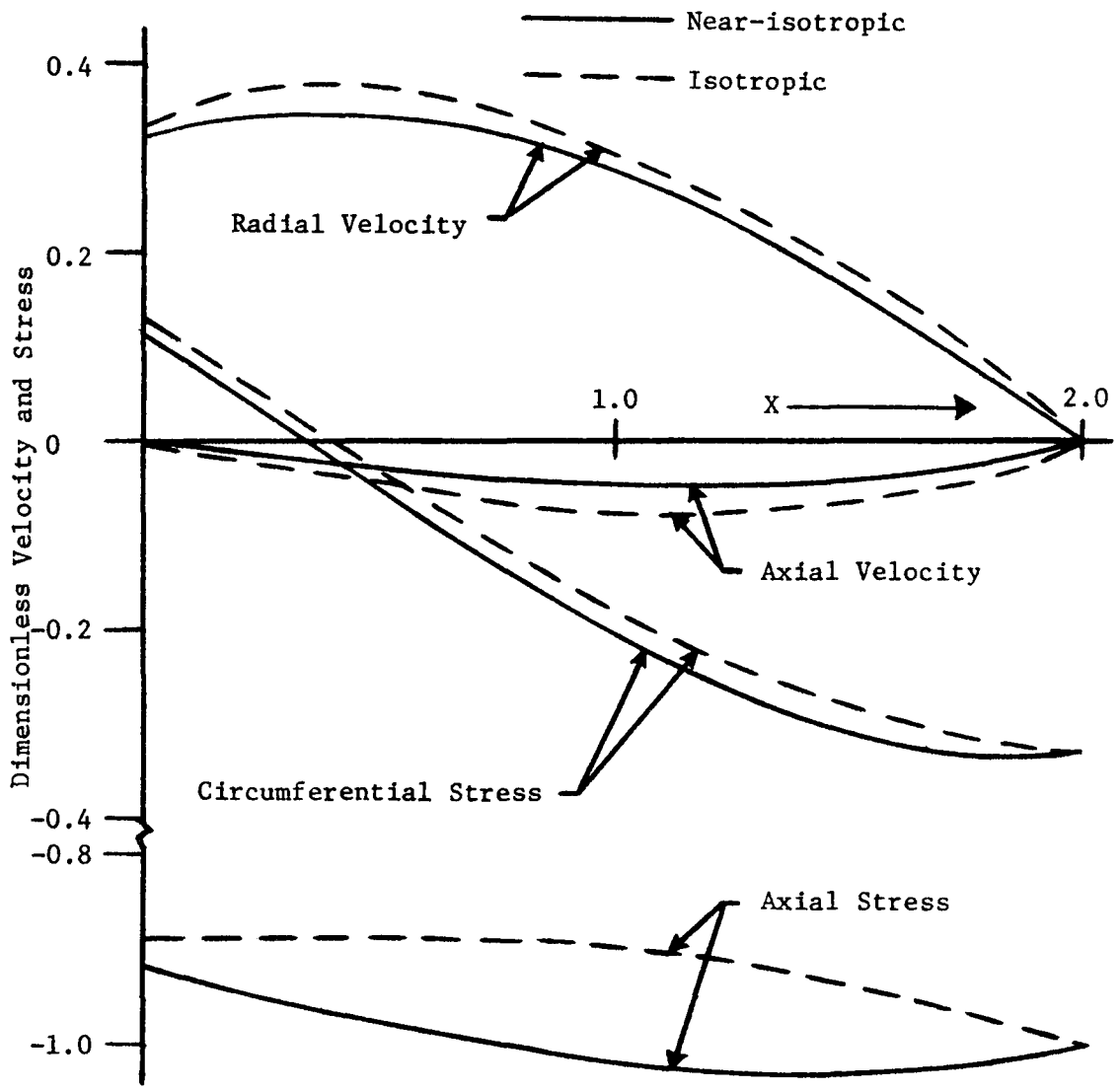

Figure 10. Comparison of results for "near-isotropic" case (θ = 1°; E_{TT}/E_{LL} = 0.99; G_{LT}/E_{LL} = 0.37; ν_{LT} = 0.333...; T = 2.0; ΔT = 0.0125) with Spillers' [1] results for an isotropic, cylindrical membrane shell.

On the other hand, if a faired curve is drawn through the oscillations, the result is invariably a jump across the s.ℓ.c. which is equal to the one predicted by equations 4.12. Such a fairing is shown in Figure 9. This procedure is followed for all the output, and the oscillations are not shown in subsequent figures.

It is not unexpected that membrane equations should have a difficult time modeling shock phenomena. However, it appears that the overall results of this formulation are a reasonable model of the dynamic response of a helically wound shell. This is certainly a positive step toward understanding the response of such an anisotropic shell. It is felt that the introduction of bending, transverse shear, and rotary inertia would obviate oscillations.

The Isotropic Case. As explained in Chapter III, this formulation will not yield solutions under isotropic conditions. If $E_{11} = E_{22} = E$ and $G = E/2(1+\nu)$ and/or $\theta = 0°$ or $90°$, the compatibility equations become indeterminate. However, if "near-isotropic" conditions are assumed, reasonable results are obtained as indicated in Figure 10. In this case, E_{11} was considered to be one percent larger than E_{22}, so that $E_{11}/E_{22} = 1.01$. Additionally, the helix angle was assumed to be 1° and $G = E_{11}/2(1+\nu)$, where $\nu = \frac{1}{3}$.

The two solutions are essentially identical at X = 2.0, the location of the primary wavefront, because the calculated jumps across the p.ℓ.c. are of almost identical magnitudes in both cases. However, the differences between them gradually become apparent as the numerical integration proceeds. In the "near isotropic" case, there is a

torsional wave with a non-dimensional wave speed of about 0.574 which has some limited effect on the behavior of the membrane.

The axial stress curve may appear, at first, to be inconsistent with the others. Nevertheless, the maximum percent difference, based upon the isotropic curve, is less than fifteen percent. This is no larger than the percent differences encountered in the other variables. The fact that the curvature of the axial stress plot is reversed from the isotropic to the "near-isotropic" case appears troublesome. However, it must be remembered that there are constraints on the values at both ends due to the imposed boundary conditions. Similar constraints on the other variables do not cause such a marked change in curvature simply because the maximum separation between the curves in each other pair is several times smaller than it is for the axial stress curves.

Assumed Material Properties. Values for three parameters (i.e. E_{22}/E_{11}, G_{12}/E_{11}, and ν_{12}) are necessary to completely specify the properties of the shell material. In all the cases presented here, one representative set of material properties has been assumed. These properties roughly approximate the values for boron-epoxy and carbon-epoxy composites given by Ashton, Halpin, and Petit [5]. It is assumed that the longitudinal Young's modulus (E_{11}) is ten times the transverse modulus (E_{22}). The value of the orthotropic shear modulus (G_{12}) is set at one-thirtieth of E_{11} and ν_{12} is specified as 0.3.

Varying the Helix Angle. Once the material properties have been assigned, the only remaining parameter, necessary to describe the

shell completely, is the helix angle defined in Chapter I. The restriction on the value of the helix angle is $0° < |\theta| < 90°$. The speeds of the compression and torsion waves vary with the helix angle. As θ approaches 0°, the dimensionless speed of the former wave should approach 1.0, since the effective modulus in the axial direction approaches E_{11}. As θ increases in value, the effective axial modulus decreases, causing the speed of the compression wave to diminish. The torsion wave is harder to characterize. One thing that can be said, however, is that it should propagate more slowly than the other disturbance.

In Figure 11, the variations of the wave speeds with helix angle are shown for the assumed material properties. The value of c_1 as θ approaches 90° is predictable from the value at 0°, since c_1 is proportional to the square root of the effective axial modulus. For $\theta = 90°$, the fibers are wrapped circumferentially and the axial modulus is E_{22}. As stated above, for $\theta = 0°$ the axial modulus is E_{11}. Thus,

$$\frac{E_{11}}{E_{22}} = 10.0 \Rightarrow \sqrt{\frac{E_{11}}{E_{22}}} \cong 3.16 \Rightarrow \frac{(c_1)_{0°}}{(c_1)_{90°}} \cong 3.16$$

Therefore, since $(c_1)_{0°} = 1.0$, the predicted value of $(c_1)_{90°}$ is about 0.316, which compares favorably with the value in Figure 11.

Three helix angles (i.e. 15°, 45°, and 75°) have been chosen for purposes of comparison. In Figure 11, it can be seen that c_1 is nearly maximal and c_2 is nearly minimal at 15°. At 45°, the values of the wave speeds are intermediate. At 75°, the value of c_1 has dropped and

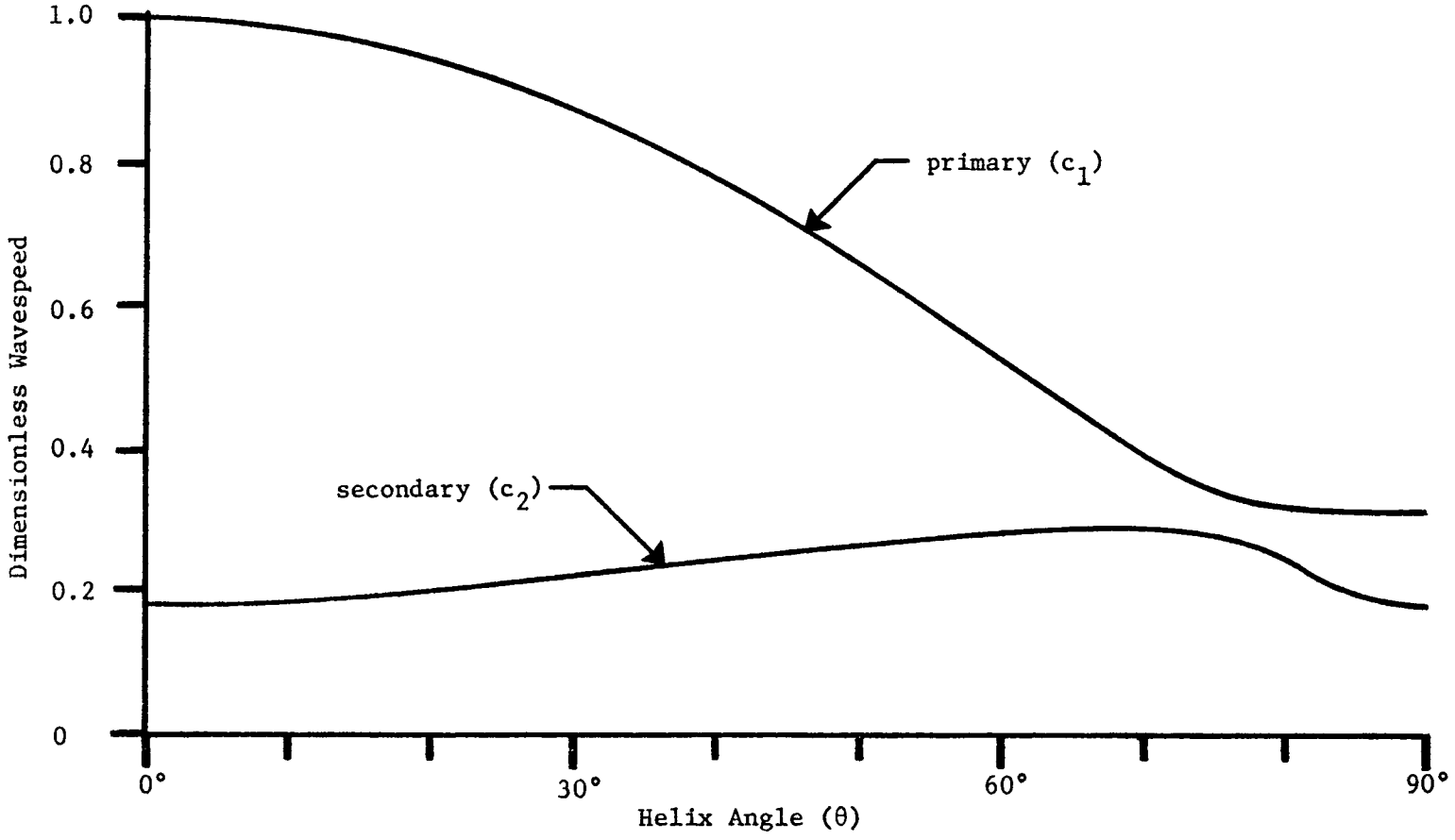

Figure 11. Variation of dimensionless wavespeeds of primary and secondary waves with helix angle for a typical composite material (E_{TT}/E_{LL} = 0.1; G_{LT}/E_{LL} = 0.0333...; ν_{LT} = 0.3).

that of c_2 has risen so that they are about at the point of closest approach.

A comparison of dimensionless circumferential velocity at T = 2.4 for the three helix angles is shown in Figure 12. It can be seen that the primary wave front (located at the extreme right of each curve) advances more rapidly, the smaller the helix angle, but that the secondary wave front slows down with decreased angle. This is as indicated by the wave speeds in Figure 11. Thus, while the primary wave has far outstripped the secondary wave for the 15° helix angle, the two wave fronts are practically coincident for the 75° configuration at the time shown. The proximity of the two disturbances in the latter case causes more pronounced gradients on either side of the torsional wave front. An additional aspect of interest is the trend of the jumps at each wave front. Across the p.ℓ.c., the jump in circumferential velocity increases as the helix angle is expanded, whereas the jump at the secondary wave front decreases under the same condition.

In Figure 13, the dimensionless shear stress parallel (and perpendicular) to the fibers is compared for the three helix angles at T = 2.4. Again, there are more pronounced gradients on either side of the s.ℓ.c. for the 75° case in which the two wave fronts are in close proximity. The nearly constant shear stress beyond the wave fronts in the 15° and 45° cases is a curious result. However, this condition does not hold for all time after T = 2.4, as is evident from the curve for S_{LT} in Figure 15.

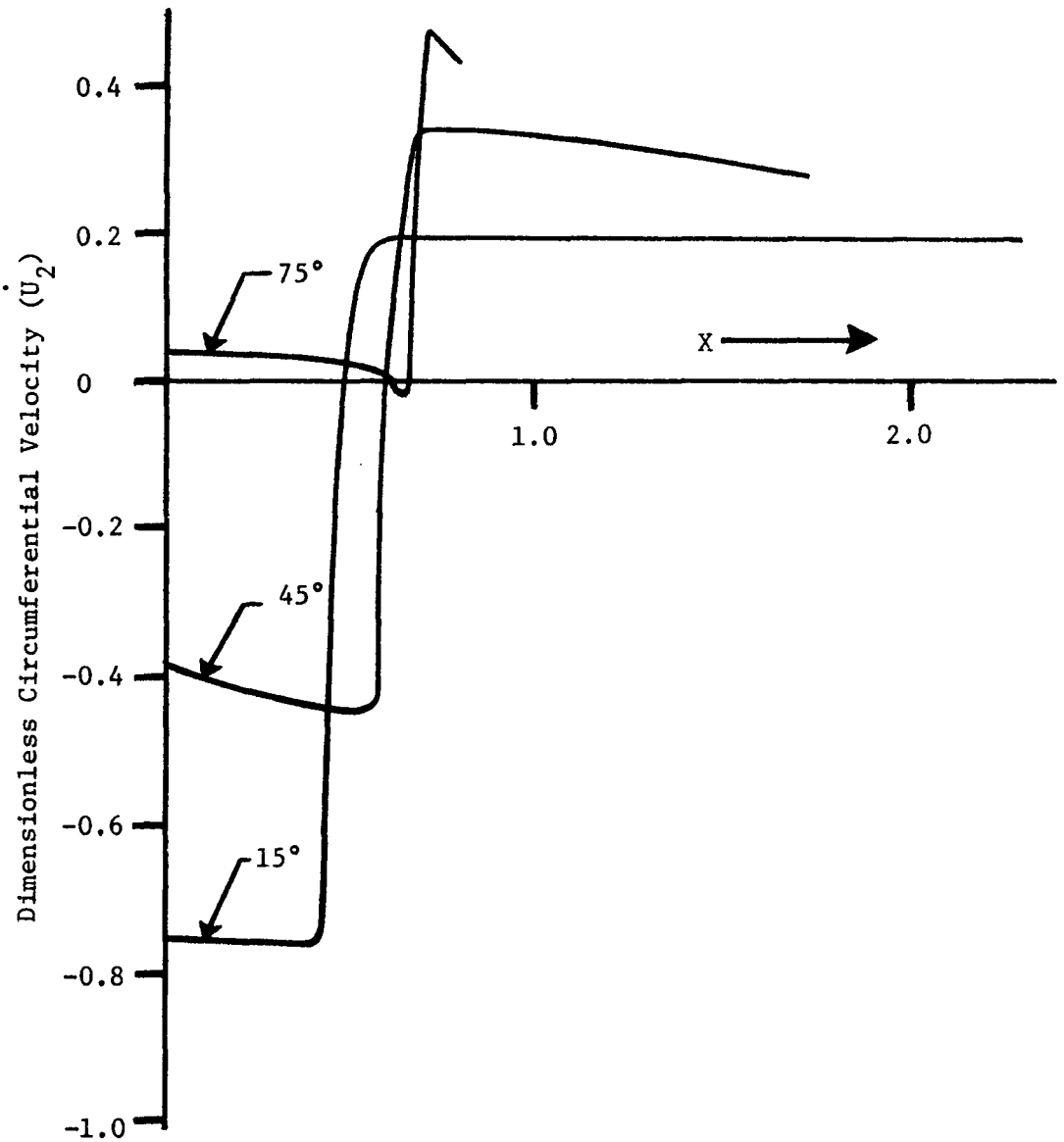

Figure 12. Spatial variation of dimensionless circumferential velocity at T = 2.4 for helix angles of 15°, 45°, and 75° (E_{TT}/E_{LL} = 0.1; G_{LT}/E_{LL} = 0.0333...; ν_{LT} = 0.3; ΔT = 0.0125).

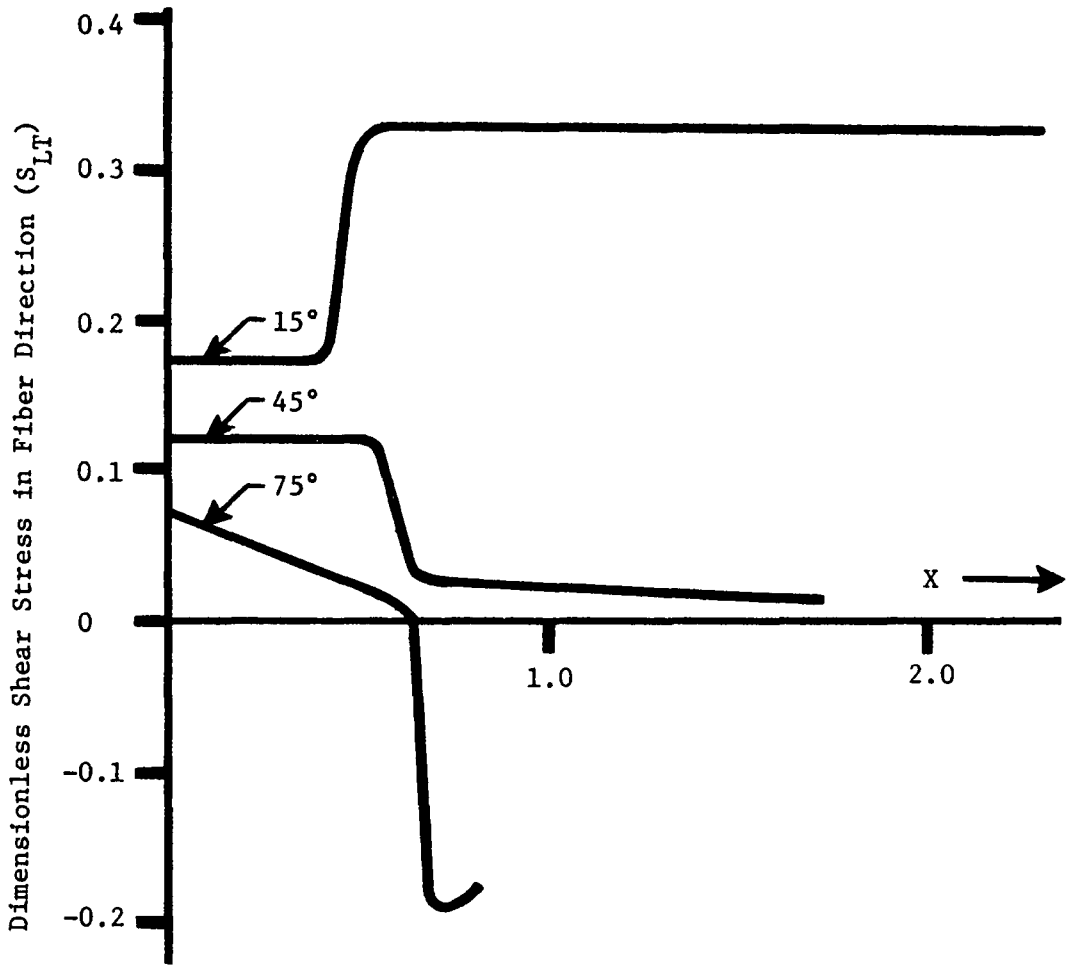

Figure 13. Spatial variation of dimensionless shear stress in fiber direction at T = 2.4 for helix angles of 15°, 45°, and 75° (E_{TT}/E_{LL} = 0.1; G_{LT}/E_{LL} = 0.0333...; ν_{LT} = 0.3; ΔT = 0.0125).

Results After a Greater Time Lapse. Considering a 45° helix angle, at T = 10.0, both wave fronts are more than two spatial units from the end of the cylinder. This means that the wave fronts have moved more than a diameter away from the wall, since x has been non-dimensionalized with respect to the cylinder radius. The spatial variations at this time have changed markedly from those presented in Figures 12 and 13.

The dimensionless velocities in the three coordinate directions are shown in Figure 14. As expected, the radial velocity does not exhibit a jump at the torsional wave front. Furthermore, the circumferential velocity changes sign as it crosses the s.ℓ.c., indicating that the direction of rotation of the shell material actually reverses from one side of the wavefront to the other.

In Figure 15, dimensionless stresses are presented. The jumps in S_T and S_{LT} across the s.ℓ.c. are very small and, in line with what was stated previously, no perceptible oscillations occurred in the output. This was not the case for S_L, which exhibits a sizable jump at the secondary wave front. At T = 10.0, the critical parameter is S_T, the stress across the fibers. Not only does this variable exhibit greater magnitudes, in both tension and compression, than the other stresses, but it is oriented in the direction of least material strength.

Conclusions

Parametric Study. It is evident that the results presented herein are not by any means complete. The number of curves which could be

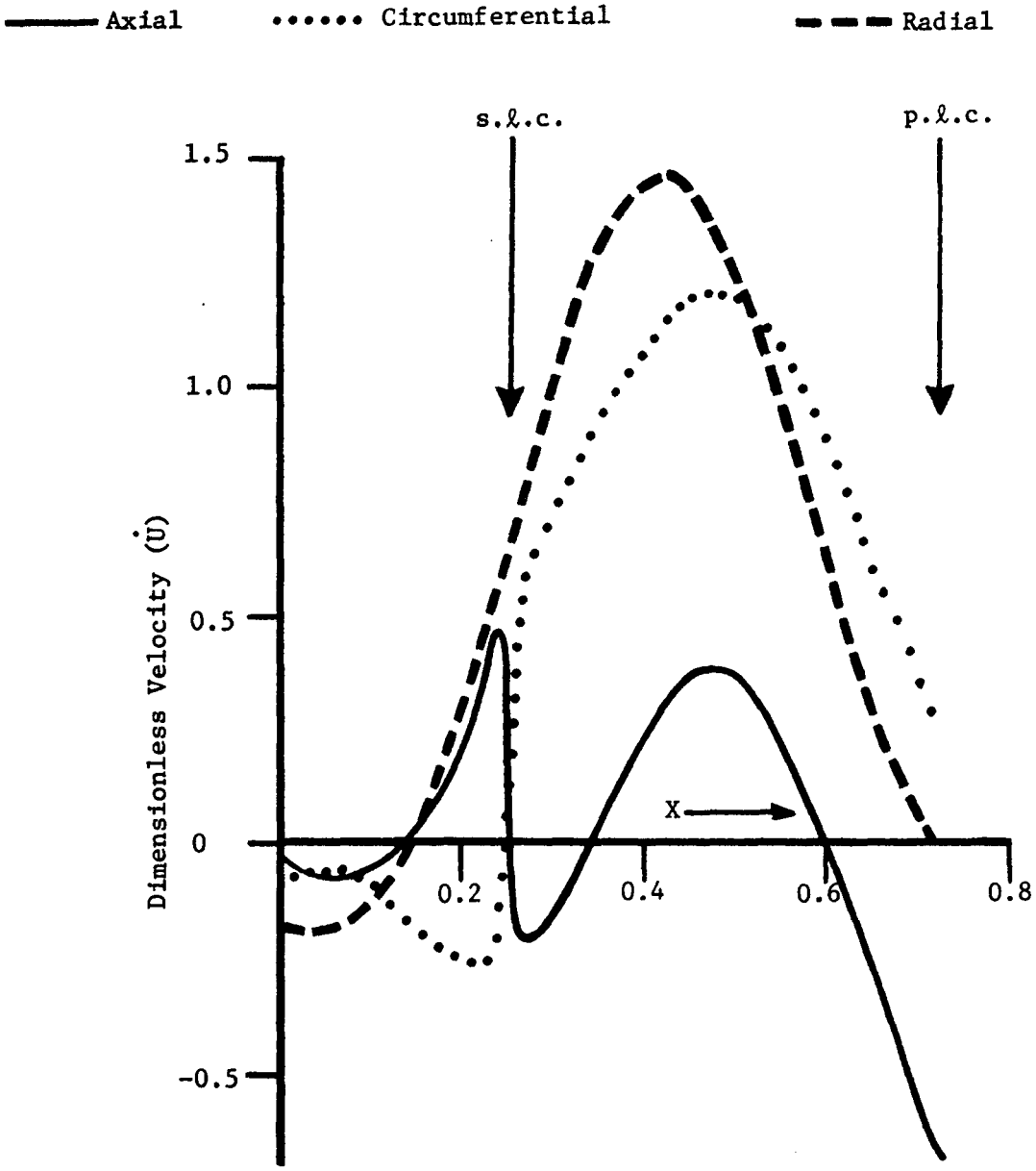

Figure 14. Spatial variation of non-dimensionalized axial, circumferential and radial velocities at T = 10.0 (θ = 45°; E_{TT}/E_{LL} = 0.1; G_{LT}/E_{LL} = 0.0333...; ν_{LT} = 0.3; ΔT = 0.025).

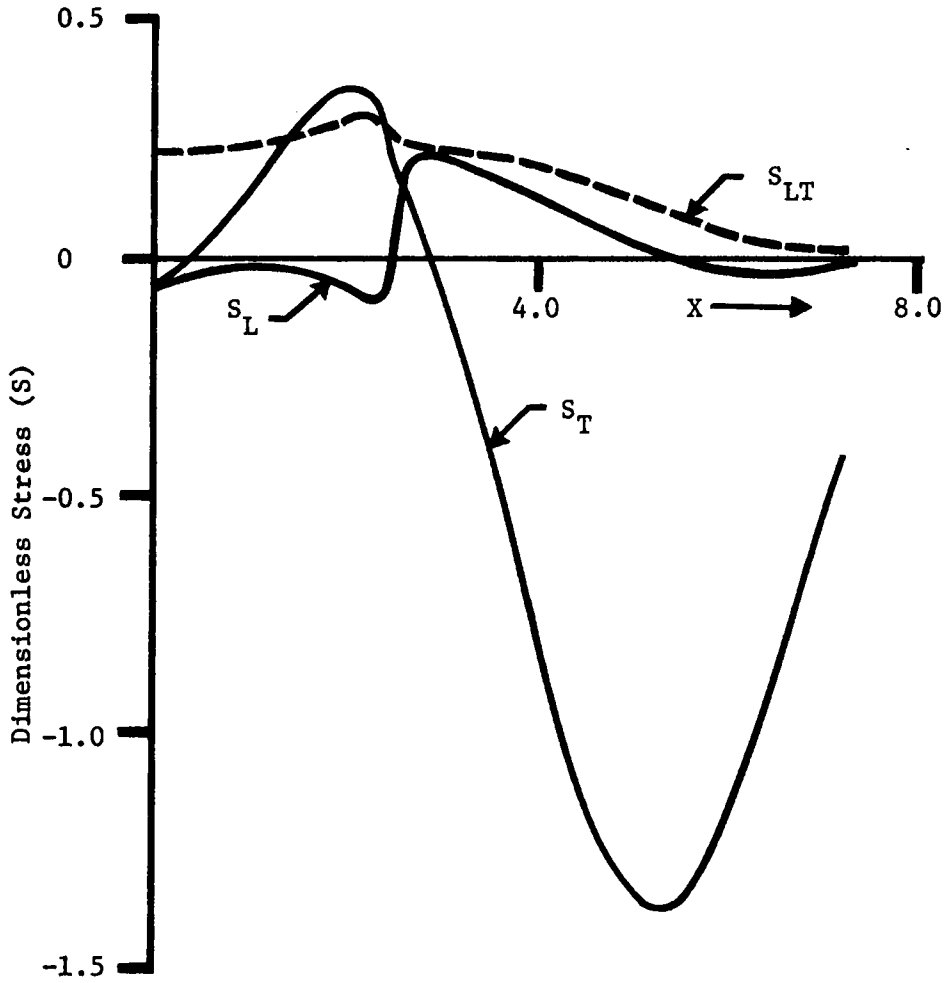

Figure 15. Spatial variation of the dimensionless stresses parallel (S_L) and perpendicular (S_T) to the fibers and of the corresponding dimensionless shear stress (S_{LT}) at T = 10.0 ($\theta = 45°$; $E_{TT}/E_{LL} = 0.1$; $G_{LT}/E_{LL} = 0.0333...$; $\nu_{LT} = 0.3$; $\Delta T = 0.025$).

developed for just one set of material properties is, of course, very large. The complete results for cases at times around T = 10.0 or beyond become voluminous, and orderly paring of the output is imperative. A parametric study should be undertaken based upon spatial and/or temporal profiles of the various parameters, possibly concentrating on stresses. Such a study is now feasible, using the computer program, HELCYD, presented in the appendix. However, further evidence is necessary to enhance the usefulness of the information provided.

Experimental Data and Rate-Dependence. Experimental data are needed to confirm or disprove the validity of the assumptions made in this analysis. Practically speaking, the problem should be extended to the cylinder of finite length before any comparisons are attempted. The method of characteristics, as developed here for the case of no reflections, should provide a convenient vehicle for introduction of reflections. A right hand wall with boundary conditions assigned must be introduced, and an additional pair of leading characteristics with reversed slopes must be added for each reflection. Thus, the p.ℓ.c.'s would form a zig-zag pattern between the walls for increasing time, and the s.ℓ.c.'s would form a similar pattern with lower frequency.

Even the assumption of a finite membrane of linearly elastic material might not yield results sufficiently close to experimental data. There are two additional factors, either or both of which might be necessary to reproduce experimental results within recognizable limits. Unless a very thin cylindrical lamina can be constructed and tested accurately using strain gages, laser techniques, holography,

or some other method, the membrane assumption may have to be expanded to consideration of a Timoshenko shell. Moreover, many composite materials are known to have rate-dependent properties. Thus, viscoelastic parameters may be necessary to provide an identifiable correlation between the numerical and experimental data. These parameters would have to be defined to fit the numerical curves to experimental results, after which additional experiments could be utilized to test the predictive capability of the numerical solution.

Tests to Determine Material Properties. Once a numerical procedure, capable of reproducing empirical results with sufficient reliability, is developed, the problem may be reversed. The numerical solution might then be employed, in conjunction with data from a helically-wound test specimen, to find material properties (including any viscoelastic parameters) of any given composite material. The potential capability for designing a procedure whereby data from one standard test specimen is used to completely specify the properties of a given composite material is perhaps one of the most important justifications for accurate numerical modeling of the dynamic response of a helically wound cylinder.

Concluding Remarks. This thesis has been undertaken with the realization that it encompasses one small step in a larger scheme. Its primary merit lies in the extension of the method of characteristics to a problem involving two superimposed wave phenomena which are generated simultaneously. This, to the author's knowledge, has not been presented previously in the literature. The concept of having a

set of equations involving the jumps at both wave fronts, which must be valid simultaneously at the origin, is new. This set of equations (4.12) includes three equations for jumps across the p.ℓ.c., three for jumps across the s.ℓ.c. and an additional two equations to account for boundary conditions at the wall. The concept could easily be expanded to a problem involving three or more superimposed wave phenomena, with the number of equations to be satisfied at the origin expanding proportionally.

Now that the jumps generated by the numerical solution at the torsional wave front and those predicted by the simultaneous equations valid at the origin have been shown to be equivalent, an alternative procedure for the numerical integration is possible. The integration can be halted just below the s.ℓ.c. The jumps calculated from the simultaneous equations can then be added to the values computed by the numerics and the resulting values assigned as boundary conditions along the s.ℓ.c. before the integration proceeds. Thereby, the problems involved in generating the steep gradients at the wave front could be circumvented.

REFERENCES

1. Spillers, W. R., "Wave Propagation in a Thin Cylindrical Shell," Journal of Applied Mechanics, Vol. 32, No. 2, Trans. ASME, Vol. 87, Series E, June 1965, pp. 346-350.

2. Counts, J. and Bennett, J. G., "Axial Wave Propagation in Membrane Shells of Revolution," International Journal for Numerical Methods in Engineering, Vol. 3, 1971, pp. 181-198.

3. Reuter, R. C., "Shear-Coupled Waves in a Thin, Helically Wrapped Cylindrical Shell," Journal of Composite Materials, Vol. 3, October 1969, pp. 676-683.

4. Chou, P. C. and Mortimer, R. W., "Solution of One-Dimensional Elastic Wave Problems by the Method of Characteristics," Journal of Applied Mechanics, Vol. 34, No. 3, September 1967, pp. 745-750.

5. Ashton, J. E., Halpin, J. C. and Petit, P. H., Primer on Composite Materials: Analysis, Technomic Publishing Company (1969).

6. Chou, P. C. and Perry, R. F., "The Classification of Partial Differential Equations in Structural Dynamics," Volume of Technical Papers on Structural Dynamics, AIAA Structural Dynamics and Aeroelasticity Specialist Conference, and the ASME/AIAA Structures, Structural Dynamics and Materials Conference, New Orleans, Louisiana, April 1969.

7. Tsai, S. W. and Pagano, N. J., "Invariant Properties of Composite Materials," Composite Materials Workshop, Technomic Publishing Company, January 1968.

8. Reuter, R. C., "Membrane Motion of a Thin, Single Layer, Generally Orthotropic, Cylindrical Shell," Journal of Composite Materials, Vol. 4, April 1970, pp. 254-263.

9. Berkowitz, Harvey M., "Longitudinal Impact of a Semi-Infinite Elastic Cylindrical Shell," Journal of Applied Mechanics, Vol. 30, Trans. ASME, Vol. 85, Series E, September 1963, pp. 347-355.

10. Testa, R. B. and Bleich, H. H., "Longitudinal Impact of the Semi-Infinite Cylindrical Viscoelastic Shell," Office of Naval Research, Project NR 064-417, Technical Report 16, Columbia University, June 1963.

11. Leonard, R. W. and Budiansky, B., "On Traveling Waves in Beams," NACA Technical Note 2874, January 1953.

APPENDIX

Program HELCYD

The computer program which produces the numerical solutions, code-named HELCYD, is written in Fortran IV for the IBM 360 system at Virginia Polytechnic Institute and State University. All floating-point variables and function subprograms are specified in double precision. All variables are floating-point, except those whose names begin with an I or a J. The program consists of an executive routine, primarily responsible for input-output, incrementing and sequencing, plus six subroutines. A complete listing is included in this appendix. Comment cards have been introduced to relate the various parts of the program to the equations and procedures developed in the text. The variable names have been made parallel to those used in the text. An abridged nomenclature, sufficient to clarify the logic of the naming system, precedes the listing.

Input

Four data cards are required to completely specify the input, as follows:

Card 1 (material properties and helix angles)

FØRMAT(6D12.5)

ERATIØ .... E_{11}/E_{22} is specified. It is inverted in the program to yield E_{22}/E_{11}

GRATIØ .... E_{11}/G_{12} is specified. It is also inverted.

GNU12 .... ν_{12}

ANGSRT; ANGFIN; ANGINT .... θ_{start}; θ_{finish}; $\theta_{interval}$ (in degrees). A group of cases, with the helix angle uniformly incremented between them, can be specified. If $\theta_{start} < \theta_{finish}$, $\theta_{interval}$ must be positive. If $\theta_{start} > \theta_{finish}$, $\theta_{interval}$ must be negative. The interval is simply added to the starting value in each successive case. When the finishing value is passed, the program stops. Therefore, there will be output at θ_{finish} only if the range between θ_{start} and θ_{finish} is evenly divisible by $\theta_{interval}$.

Card 2 (time specifications)

FØRMAT (5D12.5)

DTSRT; DTFIN; DTINT .... ΔT_{start}; ΔT_{finish}; $\Delta T_{interval}$. These parameters are specified exactly as the helix angles on card 1. The only point of distinction is that, when ΔT_{finish} is passed, the program increments θ and then begins incrementing ΔT from ΔT_{start} once again. Thus, all values of ΔT are run for each helix angle.

TMAX .... T_{max} is the upper limit of the numerical integration and is the same for all cases in a given run. If T_{max} is not evenly divisible by ΔT, the integration is carried one point beyond T_{max}.

DTDAT .... ΔT_{data} permits the reduction of voluminous output. If it is left blank, values are printed for all grid points. When a non-zero value is specified, it is divided by ΔT in each case and the result is truncated to an integer (I). Then data for every Ith row of grid points, starting with the origin, are printed.

Card 3 (banded output specifications)

FØRMAT (4D12.5)

XB1; XE1; XB2; XE2 .... Beginning and ending values of X for two bands of data. Only data for which XB1 $\leq$ X $\leq$ XE1 or XB2 $\leq$ X $\leq$ XE2 is printed. If only one band is desired, XB1 and XE1 are left blank. n.b. The options on cards 3 and 4 cannot be used simultaneously. If card 3 is used, card 4 must be left entirely blank and vice versa.

Card 4 (banded output specifications continued)

FØRMAT (4D12.5)

TB1; TE1; TB2; TE2 .... Parallel to card 3, except that bands are specified for T, not X.

Output

Values of velocities, spatial derivatives, radial displacement, and various stresses are specified for each grid point. In all, twelve variables are tabulated and their identities are clearly indicated on the output. Wave speeds, magnitudes of jumps across leading characteristics, and locations and values of stress maxima are included for each case.

Exemplary Nomenclature

Program	Text
AM	a^-

Program	Text
BP	b^{+}
C1	c_1
DT	ΔT
DTAS	ΔT^*
ETA1P	η_1^{+}
KAP1M	κ_1^{-}
LAM2P	λ_2^{+}
MU2M	μ_2^{-}
P1P	p_1^{+}
Q 11	Q_{11}
U 3	U_3
U1DØ	$\dot{U}_1$
U2PR	U_2'
U1DØLC	$(\dot{U}_1)_{p.\ell.c.}$
W1	W_1

```
      IMPLICIT REAL*8(A-H,K-Z)
      COMMON/RTS/W1,W2,W3,W4,W5,THETA,Q11,Q12,Q13,Q21,Q22,Q23,Q31,Q32,
     1Q33,CHI,UPSLON,CHUP,P2P,P1P,ETA1P,KAP1P,LAM1P,MU1P,ETA1M,KAP1M,
     2LAM1M,MU1M,ETA2P,KAP2P,LAM2P,MU2P,ETA2M,KAP2M,LAM2M,MU2M
      COMMON/PRM/ALPHA,BETA,GAMMA,ZETA,DT,DTAS,K1,K2,K3,K4,L1,L2,L3,L4,
     1L5,L6,M1,M2,M3,M4,N1,N2,N3,N4,N5,N6,KL1,KM1,KN1,KL2,KM2,KN2,KL12,
     2KM12,KN12,LN56,ML24,MN24,NL56,ML,MN,NL,NM,DX,NLT,LNT
      COMMON/BNI/R1,R2,R3,R4,R5,R6,KR1,KR2,KR12,LR56,MR24,NR56,MR,NR,
     1U3DOT,U1PRAS,U1DOAS,U2PRAS,U2DOAS,U3DOAS,U1PR,U1DO,U2PR,U2DO,U3DO,
     2U3,U1PRP,U1DOP,U2PRP,U2DOP,U3DOP
      COMMON/SPE/COSTH,SINTH,SLMAX,STMAX,SLTMAX,XSL,TSL,XST,TST,XSLT,
     1TSLT,T,TMAX,INEX,INDAT,JNDAT
      COMMON/XTB/XB1,XE1,XB2,XE2,TB1,TE1,TB2,TE2,XBE,SXT
      DIMENSION U1PR(210),U1DO(210),U2PR(210),U2DO(210),U3DO(210),
     1U3(210),U1PRP(210),U1DOP(210),U2PRP(210),U2DOP(210),U3DOP(210)
      DIMENSION A(64),B(8)
C
C     INPUT DATA ARE READ.  E11/E22 AND E11/G12 ARE INPUT AND THEN IN-
C     VERTED.  FOR A BATCH OF CASES WITH DIFFERENT HELIX ANGLES, THE
C     STARTING AND FINAL ANGLES AND INTERVAL BETWEEN ANGLES IN SUCCEED-
C     ING CASES ARE SPECIFIED.
C
      READ(5,50) ERATIO,GRATIO,GNU12,ANGSRT,ANGFIN,ANGINT
   50 FORMAT(6D12.5)
      READ(5,60) DTSRT,DTFIN,DTINT,TMAX,DTDAT
   60 FORMAT(5D12.5)
      READ(5,62) XB1,XE1,XB2,XE2,TB1,TE1,TB2,TE2
   62 FORMAT(4D12.5)
      XBE= XB1+XE1+XB2+XE2
      SXT= XBE+TB1+TE1+TB2+TE2
      ERATIO= 1.D0/ERATIO
      GRATIO= 1.D0/GRATIO
```

```
      WRITE(6,65) ERATIO,GRATIO,GNU12,TMAX
   65 FORMAT(1H1,41X,44HASSUMED NON-DIMENSIONAL MATERIAL PROPERTIES://1H
     10,37X,37HRATIO OF YOUNG'S MODULI (E22/E11)----,D14.7//1H0,22X,68HR
     2ATIO OF SHEAR MODULUS TO LONGITUDINAL YOUNG'S MODULUS (G12/E11)---
     3-,D14.7//1H0,43X,26HPOISSON'S RATIO (NU12)----,D14.7//1H0,31X,38HT
     4HIS ANALYSIS IS CARRIED UP TO TIME = ,D14.7,11H INCLUSIVE.)
C
C     W1 THROUGH W5 ARE DEFINED AS IN EQS. 2.39, EXCEPT THAT THEY HAVE,
C     IN EFFECT, BEEN DIVIDED THROUGH BY RHO*C(ZERO)**2 (NON-DIMENSION-
C     ALIZED).  THUS, THE STIFFNESSES, Q(I,J), WILL NOT HAVE TO BE DIV-
C     IDED BY THIS FACTOR WHEN THEY ARE CALCULATED IN TERMS OF THE W
C     PARAMETERS.
C
      W1= 0.125D0*(3.D0+3.D0*ERATIO+2.D0*GNU12*ERATIO+4.D0*GRATIO*(1.D0-
     1GNU12*GNU12*ERATIO))
      W2= 0.5D0*(1.D0-ERATIO)
      W3= 0.125D0*(1.D0+ERATIO-2.D0*GNU12*ERATIO-4.D0*GRATIO*(1.D0-GNU12
     1*GNU12*ERATIO))
      W4= 0.125D0*(1.D0+ERATIO+6.D0*GNU12*ERATIO-4.D0*GRATIO*(1.D0-GNU12
     1*GNU12*ERATIO))
      W5= W3+GRATIO*(1.D0-GNU12*GNU12*ERATIO)
C
C     THE HELIX ANGLE AND TIME INTERVAL ARE DEFINED AT THE BEGINNING OF
C     EACH CASE.
C
      THETAD= ANGSRT-ANGINT
   70 DT= DTSRT-DTINT
      THETAD= THETAD+ANGINT
      IF(THETAD.GT.ANGFIN) STOP
      THETA= THETAD*0.01745329251994 3D0
      COSTH= DCOS(THETA)
      SINTH= DSIN(THETA)
```

```
C
C     SUBROUTINE ROOTS CALCULATES THE ROOTS OF THE WAVE SPEED EQUATION
C     AS DEFINED IN EQS. 3.19.  IT THEN GENERATES THE COEFFICIENTS IN
C     EQS. 3.28.
C
      CALL ROOTS
C
C     WAVE SPEEDS ARE CALCULATED AS IN EQS. 4.1-2.
C
      C1= 1.D0/P1P
      C2= 1.D0/P2P
      WRITE(6,75) THETAD,C1,C2
   75 FORMAT(1H1,40X,29HTHE ASSUMED ANGLE OF WRAP IS ,F8.4,9H DEGREES.//
     1 1H0,43X,31HTHE SPEED OF THE AXIAL WAVE IS ,F8.5//1H ,41X,35HTHE SP
     2EED OF THE TORSIONAL WAVE IS ,F8.5)
C
C     THE TIME-INTERVAL IS INCREMENTED AT THE BEGINNING OF EACH NEW CASE
C
   80 DT= DT+DTINT
      DX= DT/P1P
      IF(((DT.GT.DTFIN).AND.(DTINT.GT.0.D0)).OR.((DT.LT.DTFIN).AND.(DTIN
     1T.LT.0.D0))) GO TO 70
C
C     AN INDEX, LIMITING PRINTED OUTPUT, IS DEFINED.  IT GOVERNS WHETHER
C     EVERY, EVERY SECOND, OR EVERY THIRD, ETC. VALUE IS PRINTED.
C
      INDAT= IDINT(DTDAT/(2.D0*DT))
      IF(INDAT.EQ.0) INDAT= 1
      INEX= 0
C
C     SUBROUTINE PARAMS COMPUTES A NUMBER OF INTERMEDIATE PARAMETERS
C     NEEDED IN THE DIFFERENCE EQUATIONS.
```

```
C
      CALL PARAMS
C
C     THE ELEMENTS IN THE MATRIX EQ., 4.12, ARE DEFINED.  THE (A) ARRAY
C     REPRESENTS THE COEFFICIENT MATRIX ARRANGED COLUMNWISE.  THE (B)
C     ARRAY REPRESENTS THE RIGHT HAND COLUMN VECTOR.  ALL ELEMENTS OF
C     (A) ARE ZEROED AND THEN THE NON-ZERO ONES ARE DEFINED.
C
      DO 81 J= 1,64
      A(J)= 0.D0
   81 CONTINUE
      DO 82 J= 1,8
      B(J)= 0.D0
   82 CONTINUE
      A(1)= 1.D0
      A(2)= 1.D0
      A(3)= 1.D0
      A(16)= 1.D0
      A(36)= 1.D0
      A(37)= 1.D0
      A(38)= 1.D0
      A(48)= 1.D0
      B(8)= 1.D0
      A(7)= Q31
      A(23)= Q33
      A(39)= Q31
      A(55)= Q33
      A(9)= ETA1M
      A(10)= ETA2M
      A(11)= ETA2P
      A(44)= ETA1P
      A(45)= ETA1M
```

```
      A(46)= ETA2M
      A(17)= KAP1M
      A(18)= KAP2M
      A(19)= KAP2P
      A(52)= KAP1P
      A(53)= KAP1M
      A(54)= KAP2M
      A(25)= LAM1M
      A(26)= LAM2M
      A(27)= LAM2P
      A(60)= LAM1P
      A(61)= LAM1M
      A(62)= LAM2M
      JN= 8
C
C     SUBROUTINE SEQSO SOLVES SETS OF SIMULTANEOUS EQUATIONS OF FORM
C     (A)*(X)=(B), WHERE (A) IS AN N BY N MATRIX, AND (X) AND (B) ARE
C     COLUMN VECTORS WITH N TERMS.  HERE AN 8 BY 8 SYSTEM IS INPUT.
C
      CALL SEQSO(A,B,JN,JKS)
      IF(JKS.EQ.0) GO TO 84
      WRITE(6,83)
   83 FORMAT(1H+,5X,28HTHE JUMP MATRIX IS SINGULAR )
      STOP
   84 WRITE(6,85) (B(J),J=1,8)
   85 FORMAT(1HO,2X,58HJUMPS ACROSS THE PRIMARY LEADING CHARACTERISTIC:
     1 (U1PR)= ,F9.5,10H  (U1DO)= ,F9.5,10H  (U2PR)= ,F9.5,10H  (U2DO)=
     2,F9.5,//,2X,58HJUMPS ACROSS  SECONDARY  LEADING CHARACTERISTIC:  (
     3U1PR)= ,F9.5,10H  (U1DO)= ,F9.5,10H  (U2PR)= ,F9.5,10H  (U2DO)= ,F
     49.5)
      U1DOLC= -1.D0+B(2)
      U1PRLC= B(1)
```

```
      U2PRLC= B(3)
      U2DOLC= B(4)
C
C     HEADINGS FOR THE OUTPUT ARE WRITTEN.
C
      WRITE(6,94) DT
   94 FORMAT(1H1,48X,21HTHE TIME INTERVAL IS ,F9.6/1H ,69X,9H---------)
      WRITE(6,500)
  500 FORMAT(1H0,126H**********************************************************
     1**********************************************************************
     2*********/)
      WRITE(6,95)
   95 FORMAT(1H+,9H  AXIAL  ,3H : ,9H ELAPSED ,3H : ,14H    AXIAL     ,3
     XH : ,14H    AXIAL     ,                                              2
     1H :,15HCIRCUMFERENTIAL,2H :,15HCIRCUMFERENTIAL,3H : ,14H    RADIAL
     2    ,3H : ,14H    RADIAL    /1H ,10HCOORDINATE,2H: ,9H  TIME   ,3H
     3 : ,14H   SPATIAL    ,3H : ,14H   VELOCITY   ,3H : ,14H   SPATIAL
     4   ,3H : ,14H   VELOCITY   ,3H : ,14H   VELOCITY   ,3H : ,14H DISP
     5LACEMENT /1H ,9X,3H : ,9X,3H : ,14H  DERIVATIVE  ,3H : ,14X,3H : ,
     614H  DERIVATIVE  ,3H : ,14X,3H : ,14X,3H : /1H ,9H   (X)   ,3H : ,
     79H   (T)   ,3H : ,14H    (U1PR)    ,3H : ,14H    (U1DO)    ,3H : ,
     814H    (U2PR)    ,3H : ,14H    (U2DO)    ,3H : ,14H    (U3DO)    ,
     93H : ,14H     (U3)     )
      WRITE(6,500)
      WRITE(6,96)
   96 FORMAT(1H+,9X,3H : ,9X,3H : ,14H    AXIAL     ,2H :,15HCIRCUMFEREN
     1TIAL,3H : ,14H SHEAR STRESS ,3H : ,14H LONGITUDINAL ,3H : ,14H  TR
     2ANSVERSE  ,3H : ,14H SHEAR STRESS /1H ,9X,3H : ,9X,3H : ,14H    ST
     3RESS    ,3H : ,14H    STRESS    ,2H :,15H(AXIAL-         ,3H : ,14
     4H    STRESS    ,3H : ,14H    STRESS    ,3H : ,14H(LONGITUDINAL-/1H
     5 ,9X,3H : ,9X,3H : ,14X,3H : ,14X,2H :,16HCIRCUMFERENTIAL),2H: ,14
     6H(ALONG FIBERS),2H :,15H(ACROSS FIBERS),3H : ,14H TRANSVERSE)  /1H
```

```
     7 ,9X,3H : ,9X,3H : ,14H      (S1)      ,3H : ,14H      (S2)      ,3H :
     8 ,14H     (S12)      ,3H : ,14H      (SL)      ,3H : ,14H      (ST)
     9 ,3H : ,14H     (SLT)      )
       WRITE(6,500)
       IK= 0
       IMAX= 0
C
C      STRESS MAXIMA VARIABLES ARE ZEROED.
C
       SLMAX= 0
       STMAX= 0
       SLTMAX= 0
       I= 1
C
C      VALUES ARE DEFINED AT THE ORIGIN TO PREPARE FOR INTEGRATION IN
C      THE ORDER SHOWN IN FIG. 7.
C
       U1DO(1)= U1DOLC
       U1PR(1)= U1PRLC
       U2DO(1)= U2DOLC
       U2PR(1)= U2PRLC
       U3DO(1)= 0.D0
       U3(1)= 0.D0
C
C      SUBROUTINE SIGEP IS CALLED FOR EACH GRID POINT.  IT CALCULATES THE
C      STRESSES FROM THE FIRST DERIVATIVES AND RADIAL DISPLACEMENT, MONI-
C      TORS THE STRESS MAXIMA, INCREMENTS X AND T, AND GOVERNS PRINT-OUT.
C
       CALL SIGEP(I,IK,IMAX)
       I= 2
C
C      THE SAME VALUES ARE ASSIGNED AT (2) AS AT (1)(SHOWN IN FIG. 7),
```

```
C      SINCE THEY ARE BOTH ON THE P.L.C.
C
       U1DO(2)= U1DO(1)
       U1PR(2)= U1PR(1)
       U2DO(2)= U2DO(1)
       U2PR(2)= U2PR(1)
       U3DO(2)= U3DO(1)
       U3(2)= U3(1)
C
C      SUBROUTINE BOUND PERFORMS THE CALCULATIONS FOR TRIANGLES ON THE
C      BOUNDARY (FIG.6).
C
       CALL BOUND
       CALL SIGEP(I,IK,IMAX)
C
C      SUBSCRIPT ASSOCIATED WITH POINT M IN FIG.7 IS COMPUTED.  AFTER
C      POINT M, SUBSEQUENT DIAGONALS OF GRID POINTS ARE TERMINATED AT THE
C      UPPER BOUND DEFINED BY TMAX, NOT AT THE ORDINATE.  ALSO, SUBSCRIPT
C      ING WILL BE SHIFTED FOR THESE DIAGONALS TO CONSERVE COMPUTER SPACE
C
   98  TM= TMAX/DT
       TN= TM+0.999999D0
       JTMAX= IDINT(TM)
       JTNAX= IDINT(TN)
       IF(JTMAX.NE.JTNAX) JTMAX= JTMAX+1
       IF(JTMAX/2*2.LT.JTMAX) JTMAX= JTMAX+1
       IMAX= JTMAX/2+1
C
C      THE DO LOOP ENDING AT 110 CARRIES THE INTEGRATION UP TO POINT M
C      (FIG. 7).
C
       DO 110 I=3,IMAX
```

```
      U1DO(I)= U1DO(I-1)
      U1PR(I)= U1PR(I-1)
      U2DO(I)= U2DO(I-1)
      U2PR(I)= U2PR(I-1)
      U3DO(I)= U3DO(I-1)
      U3(I)= U3(I-1)
      IP= I
      IN= I-2
      DO 100 J=1,IN
      IP= IP-1
      IF(J.EQ.1) IL=1
C
C     SUBROUTINE INTER PERFORMS THE CALCULATIONS FOR INTERIOR QUADRAN-
C     GLES (FIG. 5).
C
      CALL INTER(IP,IL)
      IL= 0
  100 CONTINUE
      U2DOT= U2DO(1)
      CALL BOUND
      CALL SIGEP(I,IK,IMAX)
  110 CONTINUE
      I= IMAX
      IP= IMAX-1
      IN= IMAX-2
      IQ= IP-2
      IK= 2
C
C     SUBSCRIPTING IS SHIFTED BY ONE AT THE BEGINNING OF EACH DIAGONAL
C     AFTER POINT M (FIG. 7).
C
      DO 150 J= 1,IN
```

```
      DO 120 JR= J,IP
      U1PR(JR)= U1PR(JR+1)
      U1DO(JR)= U1DO(JR+1)
      U2PR(JR)= U2PR(JR+1)
      U2DO(JR)= U2DO(JR+1)
      U3DO(JR)= U3DO(JR+1)
      U3(JR)= U3(JR+1)
  120 CONTINUE
      IF(J.GT.IQ) GO TO 135
      DO 130 JR= J,IQ
      U1PRP(JR)= U1PRP(JR+1)
      U1DOP(JR)= U1DOP(JR+1)
      U2PRP(JR)= U2PRP(JR+1)
      U2DOP(JR)= U2DOP(JR+1)
      U3DOP(JR)= U3DOP(JR+1)
  130 CONTINUE
  135 U1PR(IMAX)= U1PR(IMAX-1)
      U1DO(IMAX)= U1DO(IMAX-1)
      U2PR(IMAX)= U2PR(IMAX-1)
      U2DO(IMAX)= U2DO(IMAX-1)
      U3DO(IMAX)= U3DO(IMAX-1)
      U3(IMAX)= U3(IMAX-1)
      JQ= IP-J
      DO 140 JR= 1,JQ
      IF(JR.EQ.1) IL= 1
      CALL INTER(IMAX-JR,IL)
      IL= 0
  140 CONTINUE
      I= I-1
      CALL SIGEP(I,IK,IMAX)
  150 CONTINUE
      I= I-1
```

```
      CALL SIGEP(I,IK,IMAX)
C
C     THE STRESS MAXIMA ARE PRINTED AT THE END OF EACH CASE.
C
      WRITE(6,500)
      WRITE(6,170) SLMAX,XSL,TSL,STMAX,XST,TST,SLTMAX,XSLT,TSLT
  170 FORMAT(1H+,126HMAXIMUM STRESSES OCCURRING IN THE ABOVE CASE:    LO
     1NGITUDINAL = IN DIRECTION OF FIBERS    TRANSVERSE = PERPENDICULAR
     2TO FIBERS///19X,36HTHE MAXIMUM LONGITUDINAL STRESS WAS ,D14.7,8H A
     3T X = ,F9.5,12H AND TIME = ,F9.5,1H.//20X,34HTHE MAXIMUM TRANSVERS
     4E STRESS WAS ,D14.7,8H AT X = ,F9.5,12H AND TIME = ,F9.5,1H.//10X,
     555HTHE MAXIMUM SHEAR STRESS (LONGITUDINAL-TRANSVERSE) WAS ,D14.7,8
     6H AT X = ,F9.5,12H AND TIME = ,F9.5,1H.)
      WRITE(6,500)
      GO TO 80
      END
```

```
      SUBROUTINE ROOTS
      IMPLICIT REAL*8(A-H,K-Z)
      COMMON/RTS/W1,W2,W3,W4,W5,THETA,Q11,Q12,Q13,Q21,Q22,Q23,Q31,Q32,
     1Q33,CHI,UPSLON,CHUP,P2P,P1P,ETA1P,KAP1P,LAM1P,MU1P,ETA1M,KAP1M,
     2LAM1M,MU1M,ETA2P,KAP2P,LAM2P,MU2P,ETA2M,KAP2M,LAM2M,MU2M
C
C     ROOTS OF THE WAVE SPEED EQUATION, STIFFNESS COEFFICIENTS, AND
C     COEFFICIENTS IN THE COMPATIBILITY RELATIONS ARE PRODUCED IN THIS
C     SUBROUTINE.
C
      C2TH= DCOS(2.D0*THETA)
      C4TH= DCOS(4.D0*THETA)
      S2TH= DSIN(2.D0*THETA)
      S4TH= DSIN(4.D0*THETA)
C
C     NON-DIMENSIONAL STIFFNESS COEFFICIENTS ARE DEFINED IN TERMS OF W
C     PARAMETERS FROM MAIN.
C
      Q11= W1+W2*C2TH+W3*C4TH
      Q22= W1-W2*C2TH+W3*C4TH
      Q33= W5-W3*C4TH
      Q12= W4-W3*C4TH
      Q21= Q12
      Q13= -0.5D0*W2*S2TH-W3*S4TH
      Q31= Q13
      Q23= -0.5D0*W2*S2TH+W3*S4TH
      Q32= Q23
C
C     CHI AND UPSILON ARE DEFINED AS IN EQS. 3.17-18.
C
      CHI= 0.5D0*(Q11+Q33)
      UPSLON= 0.5D0*(Q11+Q33)/(Q11*Q33-Q13*Q13)
```

```
      IF(CHI.LE.0.D0) GO TO 120
      CHUP= 1.D0-(1.D0/(UPSLON*CHI))
      IF((CHUP.LE.0.D0).OR.(CHUP.GE.1.D0)) GO TO 120
C
C     THE VALUES OF P(1)+ AND P(2)+ ARE CALCULATED AS IN EQS. 3.19.
C
      P2P= DSQRT(UPSLON*(1.D0+DSQRT(CHUP)))
      P1P= DSQRT(UPSLON*(1.D0-DSQRT(CHUP)))
      DO 110 I=1,4
      IF(I-2) 50,60,70
   50 RT= P1P
      GO TO 100
C
C     VALUES FOR COEFFICIENTS IN EQS. 3.28 ARE GENERATED.
C
   60 ETA1P= ETA
      KAP1P= KAP
      LAM1P= LAM
      MU1P= MU
      RT= -P1P
      GO TO 100
   70 IF(I-3) 80,80,90
   80 ETA1M= ETA
      KAP1M= KAP
      LAM1M= LAM
      MU1M= MU
      RT= P2P
      GO TO 100
   90 ETA2P= ETA
      KAP2P= KAP
      LAM2P= LAM
      MU2P= MU
```

```
      RT= -P2P
  100 ETA= (RT-RT**3*Q33)/(RT*RT*Q33-1.D0)
      KAP=-(RT*RT*Q13)/(RT*RT*Q33-1.D0)
      LAM= KAP*RT
      MU= (-RT*RT*Q12+RT**4*(Q12*Q33-Q13*Q32))/(RT*RT*Q33-1.D0)
  110 CONTINUE
      ETA2M= ETA
      KAP2M= KAP
      LAM2M= LAM
      MU2M= MU
      RETURN
  120 WRITE(6,130) CHI,CHUP,Q11,Q13,Q33,W1,W2,W3,W4,W5,THETA
  130 FORMAT(//' THERE ARE NOT FOUR REAL, DISTINCT ROOTS.  CHI=',F13.6,'
     1, CHUP=',F13.6,', Q11=',F13.6,', Q13=',F13.6,//' Q33=',F13.6,', W1
     2=',F13.6,', W2=',F13.6,', W3=',F13.6,', W4=',F13.6,', W5=',F13.6,'
     3, THETA=',F13.6,/)
      STOP
      END
```

```
      SUBROUTINE PARAMS
      IMPLICIT REAL*8(A-H,K-Z)
      COMMON/RIS/W1,W2,W3,W4,W5,THETA,Q11,Q12,Q13,Q21,Q22,Q23,Q31,Q32,
     1Q33,CHI,UPSLON,CHUP,P2P,P1P,ETA1P,KAP1P,LAM1P,MU1P,ETA1M,KAP1M,
     2LAM1M,MU1M,ETA2P,KAP2P,LAM2P,MU2P,ETA2M,KAP2M,LAM2M,MU2M
      COMMON/PRM/ALPHA,BETA,GAMMA,ZETA,DT,DTAS,K1,K2,K3,K4,L1,L2,L3,L4,
     1L5,L6,M1,M2,M3,M4,N1,N2,N3,N4,N5,N6,KL1,KM1,KN1,KL2,KM2,KN2,KL12,
     2KM12,KN12,LN56,ML24,MN24,NL56,ML,MN,NL,NM,DX,NLT,LNT
C
C     VARIOUS INTERMEDIATE PARAMETERS, NECESSARY FOR THE FINITE-
C     DIFFERENCE SOLUTION ARE COMPUTED IN THIS SUBROUTINE.
C
C     PARAMETERS DEFINED IN EQS. 5.1-9 ARE CALCULATED.
C
      ALPHA= 1.D0/P2P
      ALPHA= DATAN(ALPHA)
      BETA= 1.D0/P1P
      BETA= DATAN(BETA)
      GAMMA= 3.1415926535 9D0-ALPHA-BETA
      ZETA= 2.D0*DSIN(ALPHA)*DCOS(BETA)/DSIN(GAMMA)
      DTAS= DT*(2.D0-ZETA)
C
C     SINCE THE SOLUTIONS OF EQS. 5.26 AND THOSE OF EQS. 5.36 WERE WORK-
C     ED OUT BY HAND, INTERMEDIATE QUANTITIES WERE DEFINED TO SIMPLIFY
C     THE ALGEBRA.  VALUES FOR THE LATTER ARE GENERATED BELOW.
C
      K1= ETA1P
      K2= ETA1M
      K3= ETA2P
      K4= ETA2M
      L1= KAP1P
      L2= KAP1M
```

```
L3= KAP2P
L4= KAP2M
L5= Q23/Q21*DT
L6= Q33/Q31
M1= LAM1P
M2= LAM1M
M3= LAM2P
M4= LAM2M
N1= MU1P*DT/2.D0
N2= MU1M*DT/2.D0
N3= MU2P*DTAS/2.D0
N4= MU2M*DTAS/2.D0
N5= Q22*DT*DT/Q21+1.D0/Q21
N6= Q32*DT/Q31
KL1= (K4-K3)*(K1*L2-K2*L1)-(K2-K1)*(K3*L4-K4*L3)
KM1= (K4-K3)*(K1*M2-K2*M1)-(K2-K1)*(K3*M4-K4*M3)
KN1= (K4-K3)*(K1*N2-K2*N1)-(K2-K1)*(K3*N4-K4*N3)
KL2= (K2-K1)*(L4-L3)-(K4-K3)*(L2-L1)
KM2= (K2-K1)*(M4-M3)-(K4-K3)*(M2-M1)
KN2= (K2-K1)*(N4-N3)-(K4-K3)*(N2-N1)
KL12= (K1*L2-K2*L1)/(K2-K1)
KM12= (K1*M2-K2*M1)/(K2-K1)
KN12= (K1*N2-K2*N1)/(K2-K1)
LN56= (L5*N6-L6*N5)/(L6-L5)
ML24= (M2*L4-M4*L2)/(M4-M2)
MN24= (M2*N4-M4*N2)/(M4-M2)
NL56= (N5*L6-N6*L5)/(N6-N5)
ML= KM2*KL1-KL2*KM1
MN= KM2*KN1-KN2*KM1
NL= KN2*KL1-KL2*KN1
NM= KN2*KM1-KM2*KN1
LNT= (L5*N6-L6*N5)/(L6*DT-L5)
```

```
      NLT= (N5*L6-N6*L5)/(N6*DT-N5)
      RETURN
      END
```

```
      SUBROUTINE SEQSO(A,B,JN,JKS)
      IMPLICIT REAL*8(A-H,K-Z)
      DIMENSION A(64),B(8)
C
C     A SET OF N EQUATIONS IN N UNKNOWNS IS SOLVED IN THIS SUBROUTINE.
C
C     FORWARD SOLUTION
      TOL= 0.D0
      JKS= 0
      JJ= -JN
      DO 65 J= 1,JN
      JY= J+1
      JJ= JJ+JN+1
      BIGA= 0.D0
      IT= JJ-J
      DO 30 I= J,JN
C     SEARCH FOR MAXIMUM COEFFICIENT IN COLUMN
      IJ= IT+I
      IF(DABS(BIGA)-DABS(A(IJ))) 20,30,30
   20 BIGA= A(IJ)
      IMAX= I
   30 CONTINUE
C     TEST FOR PIVOT LESS THAN TOLERANCE (SINGULAR MATRIX)
      IF(DABS(BIGA)-TOL) 35,35,40
   35 JKS= 1
      RETURN
C     INTERCHANGE ROWS IF NECESSARY
   40 I1= J+JN*(J-2)
      IT= IMAX-J
      DO 50 JK= J,JN
      I1= I1+JN
      I2= I1+IT
```

```
      SAVE= A(I1)
      A(I1)= A(I2)
      A(I2)= SAVE
C     DIVIDE EQUATION BY LEADING COEFFICIENT
   50 A(I1)= A(I1)/BIGA
      SAVE= B(IMAX)
      B(IMAX)= B(J)
      B(J)= SAVE/BIGA
C     ELIMINATE NEXT VARIABLE
      IF(J-JN) 55,70,55
   55 IQS= JN*(J-1)
      DO 65 IX= JY,JN
      IXJ= IQS+IX
      IT= J-IX
      DO 60 JX= JY,JN
      IXJX= JN*(JX-1)+IX
      JJX= IXJX+IT
   60 A(IXJX)= A(IXJX)-(A(IXJ)*A(JJX))
   65 B(IX)= B(IX)-(B(J)*A(IXJ))
C     BACK SOLUTION
   70 JNY= JN-1
      IT= JN*JN
      DO 80 J= 1,JNY
      IA= IT-J
      IB= JN-J
      IC= JN
      DO 80 JK= 1,J
      B(IB)= B(IB)-A(IA)*B(IC)
      IA= IA-JN
   80 IC= IC-1
      RETURN
      END
```

```
      SUBROUTINE BOUND
      IMPLICIT REAL*8(A-H,K-Z)
      COMMON/RTS/W1,W2,W3,W4,W5,THETA,Q11,Q12,Q13,Q21,Q22,Q23,Q31,Q32,
     1Q33,CHI,UPSLON,CHUP,P2P,P1P,ETA1P,KAP1P,LAM1P,MU1P,ETA1M,KAP1M,
     2LAM1M,MU1M,ETA2P,KAP2P,LAM2P,MU2P,ETA2M,KAP2M,LAM2M,MU2M
      COMMON/PRM/ALPHA,BETA,GAMMA,ZETA,DT,DTAS,K1,K2,K3,K4,L1,L2,L3,L4,
     1L5,L6,M1,M2,M3,M4,N1,N2,N3,N4,N5,N6,KL1,KM1,KN1,KL2,KM2,KN2,KL12,
     2KM12,KN12,LN56,ML24,MN24,NL56,ML,MN,NL,NM,DX,NLT,LNT
      COMMON/BNI/R1,R2,R3,R4,R5,R6,KR1,KR2,KR12,LR56,MR24,NR56,MR,NR,
     1U3DOT,U1PRAS,U1DOAS,U2PRAS,U2DOAS,U3DOAS,U1PR,U1DO,U2PR,U2DO,U3DO,
     2U3,U1PRP,U1DOP,U2PRP,U2DOP,U3DOP
      DIMENSION U1PR(210),U1DO(210),U2PR(210),U2DO(210),U3DO(210),
     1U3(210),U1PRP(210),U1DOP(210),U2PRP(210),U2DOP(210),U3DOP(210)
C
C     CALCULATIONS FOR TRIANGLES ON THE BOUNDARY ARE PERFORMED IN THIS
C     SUBROUTINE (SEE FIG. 6).
C
      U1PRP(1)= U1PR(1)
      U1DOP(1)= U1DO(1)
      U2PRP(1)= U2PR(1)
      U2DOP(1)= U2DO(1)
      U3DOP(1)= U3DO(1)
C
C     R PARAMETERS FOR THE RIGHT HAND SIDE OF EQS. 5.36 ARE COMPUTED.
C
      R2= U1PR(2)+ETA1M*U1DO(2)+KAP1M*U2PR(2)+LAM1M*U2DO(2)-MU1M/2.D0*DT
     1*U3DO(2)
C
C     EQS. 5.10-11 ARE USED TO LINEARLY INTERPOLATE, TO FIND VALUES AT
C     THE ASTERISKED POINT IN FIG. 6.
C
      U1PRAS= U1PR(1)+ZETA*(U1PR(2)-U1PR(1))
```

```
      U1DOAS= U1DO(1)+ZETA*(U1DO(2)-U1DO(1))
      U2PRAS= U2PR(1)+ZETA*(U2PR(2)-U2PR(1))
      U2DOAS= U2DO(1)+ZETA*(U2DO(2)-U2DO(1))
      U3DOAS= U3DO(1)+ZETA*(U3DO(2)-U3DO(1))
      R4= U1PRAS+ETA2M*U1DOAS+KAP2M*U2PRAS+LAM2M*U2DOAS-MU2M/2.D0*DTAS*
     1U3DOAS
      R5= -U1PR(1)*DT-Q23/Q21*DT*U2PR(1)+(1.D0/Q21-Q22/Q21*DT*DT)*
     1U3DO(1)-2.D0*Q22/Q21*DT*U3(1)
      R6= -Q32/Q31*(U3(1)+U3DO(1)*DT)
C
C     INTERMEDIATE QUANTITIES, DEFINED TO SIMPLIFY THE ALGEBRA IN THE
C     SOLUTION OF EQS. 5.36, ARE COMPUTED.
C
      MR24= (M2*R4-M4*R2)/(M4-M2)
      LR56= (L5*R6-L6*R5)/(L6-L5)
      NR56= (N5*R6-N6*R5)/(N6-N5)
      U1PR(1)= (ML24*NR56*LN56+MN24*LR56*NL56-MR24*NL56*LN56)/(NLT*LNT-
     1ML24*LNT-MN24*NLT)*(NLT*LNT)/(NL56*LN56)
      U1DO(1)= 0.D0
      U2PR(1)= U1PR(1)/NLT+NR56/NL56
      U3DOT= U3DO(1)
      U3DO(1)= U1PR(1)/LNT+LR56/LN56
      U2DO(1)= (L4-L2)/(M2-M4)*U2PR(1)+(N4-N2)/(M2-M4)*U3DO(1)-(R4-R2)/
     1(M2-M4)
      U3(1)= U3(1)+(U3DOT+U3DO(1))*DT
      RETURN
      END
```

```
      SUBROUTINE INTER(IP,IL)
      IMPLICIT REAL*8(A-H,K-Z)
      COMMON/RTS/W1,W2,W3,W4,W5,THETA,Q11,Q12,Q13,Q21,Q22,Q23,Q31,Q32,
     1Q33,CHI,UPSLON,CHUP,P2P,P1P,ETA1P,KAP1P,LAM1P,MU1P,ETA1M,KAP1M,
     2LAM1M,MU1M,ETA2P,KAP2P,LAM2P,MU2P,ETA2M,KAP2M,LAM2M,MU2M
      COMMON/PRM/ALPHA,BETA,GAMMA,ZETA,DT,DTAS,K1,K2,K3,K4,L1,L2,L3,L4,
     1L5,L6,M1,M2,M3,M4,N1,N2,N3,N4,N5,N6,KL1,KM1,KN1,KL2,KM2,KN2,KL12,
     2KM12,KN12,LN56,ML24,MN24,NL56,ML,MN,NL,NM,DX,NLT,LNT
      COMMON/BNI/R1,R2,R3,R4,R5,R6,KR1,KR2,KR12,LR56,MR24,NR56,MR,NR,
     1U3DOT,U1PRAS,U1DOAS,U2PRAS,U2DOAS,U3DOAS,U1PR,U1DO,U2PR,U2DO,U3DO,
     2U3,U1PRP,U1DOP,U2PRP,U2DOP,U3DOP
      DIMENSION U1PR(210),U1DO(210),U2PR(210),U2DO(210),U3DO(210),
     1U3(210),U1PRP(210),U1DOP(210),U2PRP(210),U2DOP(210),U3DOP(210)
C
C     CALCULATIONS FOR INTERIOR QUADRANGLES ARE PERFORMED IN THIS SUB-
C     ROUTINE (SEE FIG. 5).
C
C     R PARAMETERS FROM THE RIGHT HAND SIDE OF EQS. 5.26 ARE COMPUTED.
C
      R1= U1PR(IP-1)+ETA1P*U1DO(IP-1)+KAP1P*U2PR(IP-1)+LAM1P*U2DO(IP-1)-
     1MU1P/2.D0*DT*U3DO(IP-1)
      R2= U1PR(IP+1)+ETA1M*U1DO(IP+1)+KAP1M*U2PR(IP+1)+LAM1M*U2DO(IP+1)-
     1MU1M/2.D0*DT*U3DO(IP+1)
      R5= -U1PR(IP)*DT-Q23/Q21*DT*U2PR(IP)+(1.D0/Q21-Q22/Q21*DT*DT)*
     1U3DO(IP)-2.D0*Q22/Q21*DT*U3(IP)
      IF(IL.NE.1) GO TO 30
C
C     LINEAR INTERPOLATION MUST BE USED BETWEEN POINTS N AND M IN FIG. 5
C     IF THE QUADRANGLE LIES ON THE P.L.C.
C
      U1PRAM= U1PR(IP)+ZETA*(U1PR(IP-1)-U1PR(IP))
      U1DOAM= U1DO(IP)+ZETA*(U1DO(IP-1)-U1DO(IP))
```

```
      U2PRAM= U2PR(IP)+ZETA*(U2PR(IP-1)-U2PR(IP))
      U2DOAM= U2DO(IP)+ZETA*(U2DO(IP-1)-U2DO(IP))
      U3DOAM= U3DO(IP)+ZETA*(U3DO(IP-1)-U3DO(IP))
      R3= U1PRAM+ETA2P*U1DOAM+KAP2P*U2PRAM+LAM2P*U2DOAM-MU2P/2.D0*DTAS*
     1U3DOAM
      U1PRAS= U1PR(IP)
      U1DOAS= U1DO(IP)
      U2PRAS= U2PR(IP)
      U2DOAS= U2DO(IP)
      U3DOAS= U3DO(IP)
      R4= U1PRAS+ETA2M*U1DOAS+KAP2M*U2PRAS+LAM2M*U2DOAS-MU2M/2.D0*DTAS*
     1U3DOAS
      GO TO 60
C
C     PARABOLIC INTERPOLATION IS USED TO CALCULATE ASTERISKED QUANTITIES
C     (FIG. 5) FOR ALL QUADRANGLES NOT ON THE P.L.C. (SEE EQS. 6.1-6 AND
C     FIG. 8).
C
   30 UF1= U1PR(IP-1)
      UF2= U1PR(IP)
      UF3= U1PR(IP+1)
      UF4= U1PRM
      UF5= U1PRP(IP-1)
      DO 50 JK= 1,5
      AM= (UF4-2.D0*UF2+UF1)/2.D0
      BM= (-3.D0*UF4+4.D0*UF2-UF1)/2.D0
      CM= UF4
      AP= (UF5-2.D0*UF2+UF3)/2.D0
      BP= (-3.D0*UF5+4.D0*UF2-UF3)/2.D0
      CP= UF5
      GO TO (41,42,43,44,45),JK
   41 U1PRAM= AM*(1.D0+ZETA)**2+BM*(1.D0+ZETA)+CM
```

```
      U1PRAS= AP*(1.D0+ZETA)**2+BP*(1.D0+ZETA)+CP
      UF1= U1DO(IP-1)
      UF2= U1DO(IP)
      UF3= U1DO(IP+1)
      UF4= U1DOM
      UF5= U1DOP(IP-1)
      GO TO 50
   42 U1DOAM= AM*(1.D0+ZETA)**2+BM*(1.D0+ZETA)+CM
      U1DOAS= AP*(1.D0+ZETA)**2+BP*(1.D0+ZETA)+CP
      UF1= U2PR(IP-1)
      UF2= U2PR(IP)
      UF3= U2PR(IP+1)
      UF4= U2PRM
      UF5= U2PRP(IP-1)
      GO TO 50
   43 U2PRAM= AM*(1.D0+ZETA)**2+BM*(1.D0+ZETA)+CM
      U2PRAS= AP*(1.D0+ZETA)**2+BP*(1.D0+ZETA)+CP
      UF1= U2DO(IP-1)
      UF2= U2DO(IP)
      UF3= U2DO(IP+1)
      UF4= U2DOM
      UF5= U2DOP(IP-1)
      GO TO 50
   44 U2DOAM= AM*(1.D0+ZETA)**2+BM*(1.D0+ZETA)+CM
      U2DOAS= AP*(1.D0+ZETA)**2+BP*(1.D0+ZETA)+CP
      UF1= U3DO(IP-1)
      UF2= U3DO(IP)
      UF3= U3DO(IP+1)
      UF4= U3DOM
      UF5= U3DOP(IP-1)
      GO TO 50
   45 U3DOAM= AM*(1.D0+ZETA)**2+BM*(1.D0+ZETA)+CM
```

```
      U3DOAS= AP*(1.D0+ZETA)**2+BP*(1.D0+ZETA)+CP
   50 CONTINUE
      R3= U1PRAM+ETA2P*U1DOAM+KAP2P*U2PRAM+LAM2P*U2DOAM-MU2P/2.D0*DTAS*
     1U3DOAM
      R4= U1PRAS+ETA2M*U1DOAS+KAP2M*U2PRAS+LAM2M*U2DOAS-MU2M/2.D0*DTAS*
     1U3DOAS
      U1PRP(IP)= U1PR(IP)
      U1DOP(IP)= U1DO(IP)
      U2PRP(IP)= U2PR(IP)
      U2DOP(IP)= U2DO(IP)
      U3DOP(IP)= U3DO(IP)
   60 U1PRM= U1PR(IP)
      U1DOM= U1DO(IP)
      U2PRM= U2PR(IP)
      U2DOM= U2DO(IP)
      U3DOM= U3DO(IP)
C
C     INTERMEDIATE QUANTITIES, DEFINED TO SIMPLIFY THE ALGEBRA IN THE
C     SOLUTIONS OF EQS. 5.26, ARE COMPUTED.
C
      KR1= (K4-K3)*(K1*R2-K2*R1)-(K2-K1)*(K3*R4-K4*R3)
      KR2= (K2-K1)*(R4-R3)-(K4-K3)*(R2-R1)
      KR12= (K1*R2-K2*R1)/(K2-K1)
      MR= KM2*KR1-KR2*KM1
      NR= KN2*KR1-KR2*KN1
      U2PR(IP)= (R5-DT*(KM12*NR/NM+KN12*MR/MN-KR12)-N5*MR/MN)/(DT*(KL12-
     1KM12*NL/NM-KN12*ML/MN)-N5*ML/MN+L5)
      U1PR(IP)= (KL12-KM12*NL/NM-KN12*ML/MN)*U2PR(IP)+KM12*NR/NM+KN12*MR
     1/MN-KR12
      U1DO(IP)= ((L2-L1)/(K1-K2)-(M2-M1)*NL/((K1-K2)*NM)-(N2-N1)*ML/((K1
     1-K2)*MN))*U2PR(IP)+(M2-M1)*NR/((K1-K2)*NM)+(N2-N1)*MR/((K1-K2)*MN)
     2-(R2-R1)/(K1-K2)
```

```
U2DO(IP)= -NL*U2PR(IP)/NM+NR/NM
U3DOT= U3DO(IP)
U3DO(IP)= -ML*U2PR(IP)/MN+MR/MN
U3(IP)= U3(IP)+(U3DOT+U3DO(IP))*DT
RETURN
END
```

```
      SUBROUTINE SIGEP(I,IK,IMAX)
      IMPLICIT REAL*8(A-H,K-Z)
      COMMON/RTS/W1,W2,W3,W4,W5,THETA,Q11,Q12,Q13,Q21,Q22,Q23,Q31,Q32,
     1Q33,CHI,UPSLON,CHUP,P2P,P1P,ETA1P,KAP1P,LAM1P,MU1P,ETA1M,KAP1M,
     2LAM1M,MU1M,ETA2P,KAP2P,LAM2P,MU2P,ETA2M,KAP2M,LAM2M,MU2M
      COMMON/PRM/ALPHA,BETA,GAMMA,ZETA,DT,DTAS,K1,K2,K3,K4,L1,L2,L3,L4,
     1L5,L6,M1,M2,M3,M4,N1,N2,N3,N4,N5,N6,KL1,KM1,KN1,KL2,KM2,KN2,KL12,
     2KM12,KN12,LN56,ML24,MN24,NL56,ML,MN,NL,NM,DX,NLT,LNT
      COMMON/BNI/R1,R2,R3,R4,R5,R6,KR1,KR2,KR12,LR56,MR24,NR56,MR,NR,
     1U3DOT,U1PRAS,U1DOAS,U2PRAS,U2DOAS,U3DOAS,U1PR,U1DO,U2PR,U2DO,U3DO,
     2U3,U1PRP,U1DOP,U2PRP,U2DOP,U3DOP
      COMMON/SPE/COSTH,SINTH,SLMAX,STMAX,SLTMAX,XSL,TSL,XST,TST,XSLT,
     1TSLT,T,TMAX,INEX,INDAT,JNDAT
      COMMON/XTB/XB1,XE1,XB2,XE2,TB1,TE1,TB2,TE2,XBE,SXT
      DIMENSION U1PR(210),U1DO(210),U2PR(210),U2DO(210),U3DO(210),
     1U3(210),U1PRP(210),U1DOP(210),U2PRP(210),U2DOP(210),U3DOP(210)
C
C     STRESSES AND STRESS MAXIMA ARE CALULATED, X AND T ARE INCREMENTED,
C     AND PRINT-OUT IS GOVERNED BY THIS SUBROUTINE.
C
      J= IABS(IK*IMAX-I)
      DI= DFLOAT(J)
      T= (DI-1.D0)*DT
      X= (DI-1.D0)*DX
      IF(IK.EQ.0) GO TO 40
      IM= IMAX+1
      IF(J/2*2.EQ.J) GO TO 30
      GO TO 55
   30 IM= IMAX
      T= T+DT
      X= X-DX
      GO TO 55
```

```
   40 IM= I+1
      IF(I/2*2.EQ.I) GO TO 50
      GO TO 55
   50 IM= I
      T= T+DT
      X= X-DX
   55 INEX= INEX+1
      IF(INDAT.EQ.1) GO TO 60
      JNDAT= INEX-(INEX/INDAT*INDAT)
      INK= 0
   60 DO 150 JB=1,I,2
      IQ= IM-JB
C
C     NON-DIMENSIONALIZED STRESSES ARE CALCULATED (1=PARALLEL TO AXIS/
C     2=PERPENDICULAR TO AXIS/L=TANGENT TO FIBERS, I.E. LONGITUDINAL/
C     T=NORMAL TO FIBERS, I.E. TRANSVERSE).
C
      S1= Q11*U1PR(IQ)+Q13*U2PR(IQ)+Q12*U3(IQ)
      S2= Q21*U1PR(IQ)+Q23*U2PR(IQ)+Q22*U3(IQ)
      S12= Q31*U1PR(IQ)+Q33*U2PR(IQ)+Q32*U3(IQ)
      SL= S1*COSTH*COSTH+S2*SINTH*SINTH+2.D0*S12*SINTH*COSTH
      ST= S1*SINTH*SINTH+S2*COSTH*COSTH-2.D0*S12*SINTH*COSTH
      SLT= (S2-S1)*SINTH*COSTH+S12*(COSTH*COSTH-SINTH*SINTH)
C
C     A RUNNING RECORD OF STRESS MAXIMA IS KEPT.
C
      IF(DABS(SLMAX)-DABS(SL))70,80,80
   70 SLMAX= SL
      XSL= X
      TSL= T
   80 IF(DABS(STMAX)-DABS(ST)) 90,100,100
   90 STMAX= ST
```

```
      XST= X
      TST= T
  100 IF(DABS(SLTMAX)-DABS(SLT)) 110,111,111
  110 SLTMAX= SLT
      XSLT= X
      TSLT= T
C
C     IF LIMITED OUTPUT HAS BEEN SPECIFIED, SPECIFICATIONS ARE CHECKED
C     TO SEE IF THIS DATA SHOULD BE PRINTED.  IF SO, THE WRITE STATEMENT
C     IS EXECUTED.
C
  111 IF(SXT.LT.0.0000001) GO TO 120
      IF(XBE.LT.0.0000001) GO TO 113
      IF((X.LT.XB1).OR.(X.GT.XE2)) GO TO 140
      IF((X.GT.XE1).AND.(X.LT.XB2)) GO TO 140
      IF((SXT-XBE).LT.(0.0000001)) GO TO 125
  113 IF((T.LT.TB1).OR.(T.GT.TE2)) GO TO 140
      IF((T.GT.TE1).AND.(T.LT.TB2)) GO TO 140
      GO TO 125
  120 IF(INDAT.EQ.1) GO TO 125
      IF(JNDAT.NE.1) GO TO 140
      INK= INK+1
      IF(T.GE.TMAX) GO TO 125
      IF((INK-INK/INDAT*INDAT).NE.1) GO TO 140
  125 WRITE(6,130) X,T,U1PR(IQ),U1DO(IQ),U2PR(IQ),U2DO(IQ),U3DO(IQ),
     1U3(IQ),S1,S2,S12,SL,ST,SLT
  130 FORMAT(1HO,2(F9.5,3X),6(D14.7,3X)//25X,6(D14.7,3X)/)
C
C     THE TEMPORAL AND SPATIAL COORDINATES ARE INCREMENTED.
C
  140 T= T+2.DO*DT
      X= X-2.DO*DX
```

```
150 CONTINUE
    RETURN
    END
```

The vita has been removed from the scanned document

WAVE PROPAGATION IN A SEMI-INFINITE, CYLINDRICAL, ORTHOTROPIC MEMBRANE

by

James J. Brickley, Jr.

(ABSTRACT)

A semi-infinite, cylindrical membrane of fiber-reinforced material with the fibers oriented helically along the membrane is considered. The equations of motion are written in terms of the orthotropic material properties and are solved for the condition of indeterminancy in the second derivatives of the displacements.

This produces compatibility relations, valid along characteristics in the time-space plane, and wave speed equations. Due to the fiber orientation, an extensional disturbance generates a concomitant torsional disturbance, which propagates with a slower wave speed. The solution, thus, involves two sets of superimposed characteristics.

The pertinent equations are written in finite-difference form and solved numerically. Some generalization is achieved due to non-dimensionalization of the equations. Results are presented for various fiber orientations using representative material properties. The relationship of the results to the isotropic case is also discussed. Finally, documentation of the computer program, developed for the numerical solution, is appended.